Allogeneic cell therapy from immunized donors with tumor antigen peptide enhances the antitumor effect after cyclophosphamide-using non-myeloablative allogeneic hematopoietic cell transplantation

Masumitsu Hamaguchi,[1] Masatoshi Eto,[1,5] Yoriyuki Kamiryo,[1] Ario Takeuchi,[1,2] Masahiko Harano,[1] Katsunori Tatsugami,[1] Takanori Teshima,[3] Mamoru Harada,[4] Yasunobu Yoshikai[2] and Seiji Naito[1]

[1]Department of Urology, Graduate School of Medical Sciences, Kyushu University, 3-1-1 Maidashi, Higashi-ku, Fukuoka 812-8582; [2]Division of Host Defense, Research Center for Prevention of Infectious Diseases, Medical Institute of Bioregulation, Kyushu University, 3-1-1 Maidashi, Higashi-ku, Fukuoka 812-8582; [3]Center for Cellular and Molecular Medicine, Kyushu University Hospital, 3-1-1 Maidashi, Higashi-ku, Fukuoka 812-8582; [4]Department of Immunology, Shimane University Faculty of Medicine, 89-1 Enya-cho, Izumo, Shimane 693-8501, Japan

(Received August 4, 2008/Revised September 21, 2008/Accepted September 23, 2008/Online publication November 25, 2008)

Non-myeloablative allogeneic stem cell transplantation is an option for the treatment of hematological malignancies as well as solid tumors. We recently proposed a cyclophosphamide-using non-myeloablative cell therapy in which donor lymphocytes infusion (DLI) was carried out after tolerance induction to donor cells. In this study, we tested the possibility that the cyclophosphamide-using cell therapy could be augmented by pre-immunization of donors before DLI. We initially assessed whether or not the cyclophosphamide-using cell therapy could also show antitumor effect against subcutaneously established colon 26 carcinoma. As a tumor antigen-derived peptide for colon 26, we used AH1, an immunodominant H-2L^d-binding peptide derived from the envelope protein (gp70) of an endogenous murine leukemia virus. The cyclophosphamide-using cell therapy with the DLI from donors which were pre-immunized with the AH1 peptide was compared with that from non-immunized mice. The cyclophosphamide-using cell therapy significantly suppressed subcutaneously established colon 26 carcinoma, and the tumor-rejected mice acquired the tumor-specific protective immunity. When combined with the DLI from donors that were immunized with AH1, antitumor effect of the cyclophosphamide-using cell therapy was significantly augmented. The DLI from tumor peptide-immunized donors showed no influence on donor chimerism and bodyweight of the treated mice, indicating no increased risk of graft-versus-host disease. Tumor-specific cytotoxic T lymphocytes could be generated from tumor-rejected mice. Our results indicate that the cyclophosphamide-using non-myeloablative cell therapy with the DLI from tumor peptide-immunized donors is a useful protocol to augment graft-versus-tumor effect without exacerbation of graft-versus-host disease. (*Cancer Sci* 2009; 100: 138–143)

Non-myeloablative allogeneic stem cell transplantation (SCT) is an option for the treatment of hematological malignancies as well as solid tumors.[1] Because this type of treatment is accompanied by treatment-related toxicity and mortality, a new protocol of well-tolerated non-myeloablative conditioning with fludarabine-based regimens has recently been introduced.[1–10] Nevertheless, graft-versus-host disease (GVHD) is generally inevitable in any type of non-myeloablative conditionings because mature donor T cells are the main mediators of the graft-versus-tumor (GVT) activity of this type of therapy.[11–17]

We previously reported a series of studies regarding the cyclophosphamide-induced tolerance system that comprises an i.v. injection of 1×10^8 allogeneic spleen cells (and 2×10^7 bone marrow cells) followed, usually 2 days later, by an i.p. injection of 200 mg/kg cyclophosphamide.[18,19] In this system, because the destruction of both donor-reactive T cells of host origin and host-reactive T cells of donor origin occurred in the induction phase, a stable mixed chimerism was induced.[18,19] In addition, we recently proposed a cyclophosphamide-using non-myeloablative cell therapy in which donor lymphocytes infusion (DLI) was carried out 1 day after the cyclophosphamide treatment of that tolerance-inducing system,[20] and modified the protocol to reduce the risk of GVHD while preserving the GVT activity.[21] The cyclophosphamide-using cell therapy was able to induce a significant antitumor effect against murine renal cell carcinoma, which was associated with a transient but mild degree of GVHD.

Combination of tumor-specific T-cell response with non-myeloablative allogeneic cell therapy is a reasonable idea to enhance antitumor effect. To this end, the DLI from immunized donors is an applicable method. In fact, non-myeloablative allogeneic cell therapy with the DLI from tumor cell-immunized donors was reported to be effective.[12] However, immunization of healthy donors with tumor cells hampers clinical application, and vaccination of donors with recipient-derived whole tumor cells has the risk to increase GVHD.[22] On the other hand, allogeneic bone marrow transplantation (BMT) from donors that were immunized with a model tumor antigen, influenza nucleoprotein, was reported to elicit antitumor effect *in vivo* without exacerbation of GVHD,[23] and immunization of a donor with myeloma immunoglobulin can induce tumor-specific immunity in an allogeneic BMT recipient.[24] However, the former model used a model antigen, and the latter was applied for hematological malignancy. Therefore, so far as we know, there has been no model with a real tumor antigen peptide applied for solid tumors. In addition, the above two protocols were not combined with the DLI that is responsible for the strong GVT activity. We therefore supposed that immunization of donors with tumor antigen-derived peptides, which have the potential to induce major histocompatibility complex (MHC) class I-restricted cancer-reactive cytotoxic T lymphocytes (CTL), could be an optimal method to provide the DLI with tumor-specific T-cell immunity. So far, a number of CTL-inducing antigenic peptides have been identified,[25] and their safety in the clinical setting has been well verified. In this study, we compared the antitumor effect of the cyclophosphamide-using cell therapy with the DLI from either tumor cell-immunized or tumor peptide-immunized donors.

[5]To whom correspondence should be addressed.
E-mail: etom@uro.med.kyushu-u.ac.jp

doi: 10.1111/j.1349-7006.2008.01014.x

As a result, we found that the cyclophosphamide-using non-myeloablative cell therapy with the DLI from tumor peptide-immunized donors can significantly augment GVT effect without changing the risk of GVHD.

Materials and Methods

Animals. Female BALB/c (H-2^d) recipient mice and female DBA/2 (H-2^d) donor mice were obtained from Charles River Laboratories Japan (Yokohama, Japan) at 8 weeks of age. All mice were kept in specific pathogen-free conditions and then were used for experiments at 10 weeks of age. All animal protocols were approved by the University Committee on the Use and Care of Animals at Kyushu University.

Tumors. Colon 26 and RENCA are colon carcinoma and renal cell carcinoma of BALB/c origin, respectively. P815 is a mastocytoma cell line derived from DBA/2 mice. All of them are maintained *in vitro* in a complete medium. RPMI-1640 (Gibco, Grand Island, NY, USA), supplemented with 10% heat-inactivated fetal calf serum (HyClone, Logan, UT, USA), 5×10^{-5} M 2-mercaptoethanol, 20 mM HEPES, 30 μg/mL Gentamycin (Schering Corporation, Kenilworth, NJ, USA) and 0.2% sodium bicarbonate was used as the complete medium.

Measurement of tumor growth *in vivo*. After s.c. tumor inoculation, tumor growth was inspected every 3 or 4 days by measuring the largest perpendicular diameters with a caliper which was thus recorded as the tumor area (mm^2).

Cancer treatment protocol. To evaluate the *in vivo* antitumor activity, BALB/c mice were injected s.c. with 2×10^5 colon 26 cells. Considering the clinical application, we started the cancer treatment after establishing the injected tumors (usually 7 days after tumor inoculation). Initially, 1.0 mL of the RPMI medium containing a set quantity of a mixture of 1×10^8 spleen cells and 2.0×10^7 bone marrow cells originated from donor DBA/2 mice was injected i.v. into the tail vein of BALB/c mice. Cyclophosphamide (Endoxan; Shionogi, Osaka, Japan) dissolved in phosphate-buffered saline (20 mg/mL) was injected i.p. at a dose of 200 mg/kg 2 days later. Lymphocytes (1×10^7) from either naive or immunized DBA/2 mice were injected i.v. to BALB/c mice 1 day after the cyclophosphamide treatment. To inactivate tumor cells, colon 26 cells were incubated with mitomycin-C (MMC) at a dose of 100 μg/mL at 37°C for 60 min. To immunize mice with tumor cells, inactivated colon 26 cells (1×10^6 cells) were i.p. injected into DBA/2 mice twice, 14 and 7 days before the experimental usage. To immunize mice with a tumor peptide, 100 μg of peptide in complete Freund's adjuvant (CFA) was s.c. injected into DBA/2 mice twice, 14 and 7 days before the experimental usage. AH1 (SPSYVYHOF), an immunodominant H-$2L^d$-binding peptide derived from the envelope protein (gp70) of an endogenous murine leukemia virus,[26] was purchased from Genenet (Fukuoka, Japan) and diluted in dimethylsulfoxide (DMSO) until use.

Flow cytometric analysis. The expression of the lymphocyte origin from BALB/c mice or DBA/2 mice was analyzed by two-color flow cytometry using a FACScan cytometer (Bectonn Dickinson, Mountain View, CA, USA). Phycoerythrin (PE)-conjugated antimouse CD5 (Ly-1) monoclonal antibody (PharMingen International, Tokyo, Japan) and fluorescein isothiocyanate (FITC)-conjugated mouse antimouse CD5.1 (Ly-1.1) monoclonal antibody (PharMingen International) were used for the analysis of the lymphocyte origin from either BALB/c or DBA/2 mice. The labeled cells were analyzed by FACScan and fluorescence histograms were accumulated on a logarithmic scale.

Assay of cytotoxicity. Spleen cells (5×10^5 cells/well) from tumor-rejected BALB/c mice were cultured with a peptide at 20 μg/mL in the presence of interleukin (IL)-2 (50 U/mL) for 5 days. Thereafter, the cultured cells were examined for their cytotoxicity against tumor cells using a standard ^{51}Cr-release assay.[27]

Statistics. The statistical significance of the data was determined using the unpaired two-tailed Student's *t*-test. A *P*-value of less than 0.05 was considered to be statistically significant.

Results

Antitumor activity of the cyclophosphamide-using allogeneic cell therapy against colon 26 carcinoma. We previously reported that the cyclophosphamide-using allogeneic cell therapy could show antitumor effect against s.c.-established RENCA renal cell carcinoma.[20,21] Therefore, we initially determined whether or not the cyclophosphamide-using cell therapy could also show antitumor effect against s.c.-established colon 26 carcinoma. Tumor growth was obviously suppressed in the BALB/c mice that had been treated with spleen cells and bone marrow cells on day 0, cyclophosphamide on day 2, and DLI from naive DBA/2 mice on day 3 (1 day after the cyclophosphamide treatment) (Fig. 1a). In the BALB/c mice treated with either cyclophosphamide alone or spleen cells and bone marrow cells on day 0

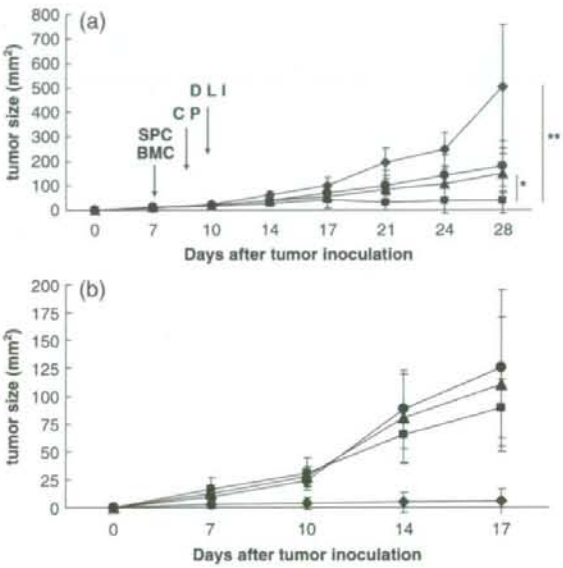

Fig. 1. Antitumor activity of the cyclophosphamide-using cell therapy against colon 26 carcinoma. (a) After establishing the injected tumors (usually 7 days after tumor inoculation), the BALB/c mice were treated as follows. (▲) Cyclophosphamide alone; (●) spleen cells (SPC) and bone marrow cells (BMC) from DBA/2 mice on day 0 and cyclophosphamide (CP) on day 2; (■) spleen cells and bone marrow cells from DBA/2 mice on day 0, cyclophosphamide on day 2, and donor lymphocytes infusion (DLI) from DBA/2 mice on day 3; (◆) untreated. Tumor growth was inspected every 3 or 4 days. The data represent the mean of five mice examined ± standard deviation (SD). The representative findings among three separate experiments are shown here. The other two experiments showed similar results. $*P < 0.01$, $**P < 0.05$. (b) BALB/c mice that had been treated with spleen cells and bone marrow cells from DBA/2 mice, cyclophosphamide, and DLI and rejected the colon 26 tumors were rechallenged with either colon 26 or RENCA tumors 120 days after the DLI. As a control tumor, RENCA was simultaneously injected on the opposite side. Tumor growth was assessed in each group. (■) Colon 26 tumors in the untreated BALB/c mice; (◆) colon 26 tumors in the tumor-rejected BALB/c mice; (●) RENCA tumors in the untreated BALB/c mice; (▲) RENCA tumors in the tumor-rejected BALB/c mice. The data represent the mean of five mice examined ± SD. The representative findings among three separate experiments are shown here. The other two experiments showed similar results.

and cyclophosphamide on day 2, tumor growth was suppressed in comparison to the untreated group, probably due to the cytotoxic effects by cyclophosphamide, but no tumor disappeared in either of the two groups. We next examined whether or not tumor-specific protective immunity was induced in the BALB/c mice that cured s.c.-established colon 26 carcinoma by the cyclophosphamide-using cell therapy. As a result, such mice completely rejected colon 26 at a rechallenge, but failed to reject RENCA renal cell carcinoma, another BALB/c syngeneic tumor (Fig. 1b). These results indicate that the cyclophosphamide-using cell therapy with the DLI from naive donors can induce antitumor effects against s.c.-established colon 26 carcinoma.

Antitumor activity of the cyclophosphamide-using cell therapy with the DLI from pre-immunized donors with tumor antigens. As described in the Introduction, the combination of tumor-specific T-cell response with the non-myeloablative allogeneic cell therapy would be a reasonable idea to enhance antitumor effect. Therefore, we next tested a hypothesis that the cyclophosphamide-using cell therapy with the DLI from donors which were pre-immunized with inactivated tumor cells could show augmented antitumor effects against colon 26 (Fig. 2a). Although the cyclophosphamide-using cell therapy with the DLI from donors which were pre-immunized with inactivated colon 26 carcinoma cells could show a slight augmentation of antitumor effect, as compared with that induced by the cyclophosphamide-using cell therapy with the DLI from non-immunized donors, there was no statistical significant difference between the two groups (Fig. 2a). In addition, although the augmentation of tumor rejection rate was apparent in the group with the DLI from donors which were pre-immunized with inactivated colon 26 carcinoma cells, as compared with that with the DLI from non-immunized donors, there was no significant difference between the two groups (Table 1).

We further tested the possibility that the cyclophosphamide-using cell therapy with the DLI from donors which were pre-immunized with a tumor antigen-derived peptide could show augmented antitumor effect on colon 26 (Fig. 2b). As a tumor antigen-derived peptide for colon 26, we used an immunodominant H-2L^d-binding peptide derived from the envelope protein (gp70) of an endogenous murine leukemia virus, designated as AH1.[26] The result was that the cyclophosphamide-using cell therapy with the DLI from donors which were pre-immunized with the AH1 peptide could show augmented antitumor effect compared to that with DLI from non-immunized mice (Fig. 2b). In addition, there was a significant difference in the tumor rejection rate between the cyclophosphamide-using cell therapy with the DLI from AH1 peptide-immunized donors and that with the DLI from control donors (Table 1).

Mixed chimerism and bodyweight in the BALB/c mice treated with the cyclophosphamide-using cell therapy with the DLI from tumor peptide-immunized donors. Chimerism was assessed in BALB/c recipients by a flow cytometric analysis of the donor (Ly-1.1$^+$) cells in the peripheral blood 10 days after the DLI. The level of donor chimerism of lymphocytes in mice treated with the cyclophosphamide-using cell therapy with the DLI from tumor peptide-immunized donors was almost same as that in those from non-immunized donors (Fig. 3a). The level of donor chimerism was sequentially assessed in these mice that survived for a long time after the rejection of colon 26 tumors, because all mice in other groups died of tumor progression. The level of donor-derived lymphocytes gradually decreased over time, and it was almost undetectable 120 days after the DLI (Fig. 3b). These results indicate that immunization of donors with a tumor peptide has no influence on chimerism of the cyclophosphamide-using cell therapy. We also sequentially assessed bodyweight as a sign of GVHD (Fig. 3c). There was no significant difference in the bodyweight between the cyclophosphamide-using cell therapy with the DLI from non-immunized donors and from tumor peptide-immunized donors (Fig. 3c), indicating no augmentation of the risk of GVHD.

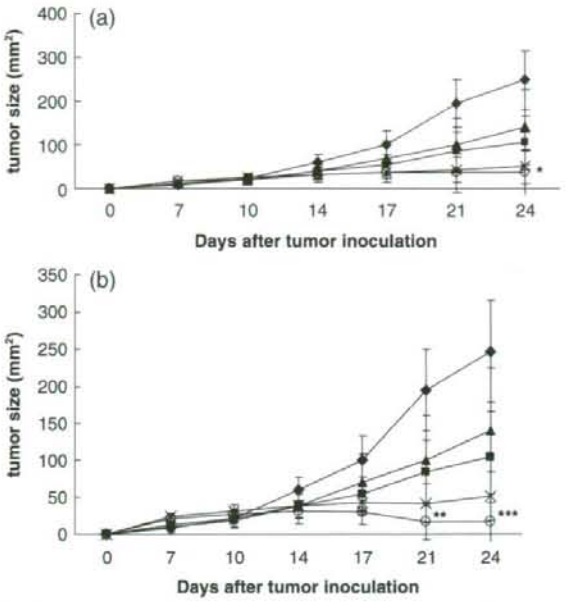

Fig. 2. Antitumor activity of the cyclophosphamide-using cell therapy against colon 26 carcinoma in combination with the donor lymphocytes infusion (DLI) from either colon 26-immunized donors or AH1 peptide-immunized donors. (a) After establishing the injected tumors (usually 7 days after tumor inoculation), the BALB/c mice were treated as follows. (■) Cyclophosphamide alone; (▲) spleen cells and bone marrow cells from DBA/2 mice on day 0 and cyclophosphamide on day 2; (X) spleen cells and bone marrow cells from DBA/2 mice on day 0, cyclophosphamide on day 2, and DLI from naive DBA/2 mice on day 3; (○) spleen cells and bone marrow cells from DBA/2 mice on day 0, cyclophosphamide on day 2, and DLI from mitomycin-C (MMC)-treated colon 26-immunized DBA/2 mice on day 3; (◆) untreated. Tumor growth was inspected every 3 or 4 days. The data represent the mean of four mice examined ± standard deviation (SD). The representative findings among three separate experiments are shown here. The other two experiments showed similar results. *P = NS. (b) After establishing the injected tumors (usually 7 days after tumor inoculation), the BALB/c mice were treated as follows. (■) Cyclophosphamide alone; (▲) spleen cells and bone marrow cells from DBA/2 mice on day 0 and cyclophosphamide on day 2; (X) spleen cells and bone marrow cells from DBA/2 mice on day 0, cyclophosphamide on day 2, and DLI from DBA/2 mice treated with complete Freund's adjuvant (CFA) alone on day 3; (○) spleen cells and bone marrow cells from DBA/2 mice on day 0, cyclophosphamide on day 2, and DLI from the AH-1 peptide-immunized DBA/2 mice on day 3; (◆) untreated. Tumor growth was inspected every 3 or 4 days. The data represent the mean of six mice examined ± SD. The representative findings among three separate experiments are shown here. The other two experiments showed similar results. **P = 0.06, ***P = 0.037.

Tumor-specific CTL in the BALB/c mice that rejected colon 26 tumors with the cyclophosphamide-using cell therapy with the DLI from tumor peptide-immunized donors. We finally determined whe-ther or not tumor-specific T-cell immunity was induced in the mice that cured s.c.-established colon 26 with the cyclophosphamide-utilizing cell therapy with the DLI from tumor peptide-immunized donors (Fig. 4). The spleen cells from colon 26-rejected BALB/c mice were stimulated *in vitro* with the AH1 peptide in the presence of IL-2, and cytolytic activity of the cultured cells was examined. As a result, the *in vitro*

doi: 10.1111/j.1349-7006.2008.01014.x

Table 1. Tumor acceptance in the mice treated with pre-immunized donor lymphocytes 24 days after tumor inoculation

	Donor SPC and BMC	CP	Pre-immunization	Mice without tumor/All mice of donor lymphocytes
Experiment 1	+	+	–	3/12
	+	+	MMC-colon 26	6/12**
Experiment 2	+	+	CFA alone	3/18
	+	+	CFA + AH1†	9/18***

†AH1 (SPSYVYHOF) peptide derived from gp70 protein. **P = 0.21, ***P = 0.03. BMC, bone marrow cells; CP, cyclophosphamide; SPC, spleen cells.

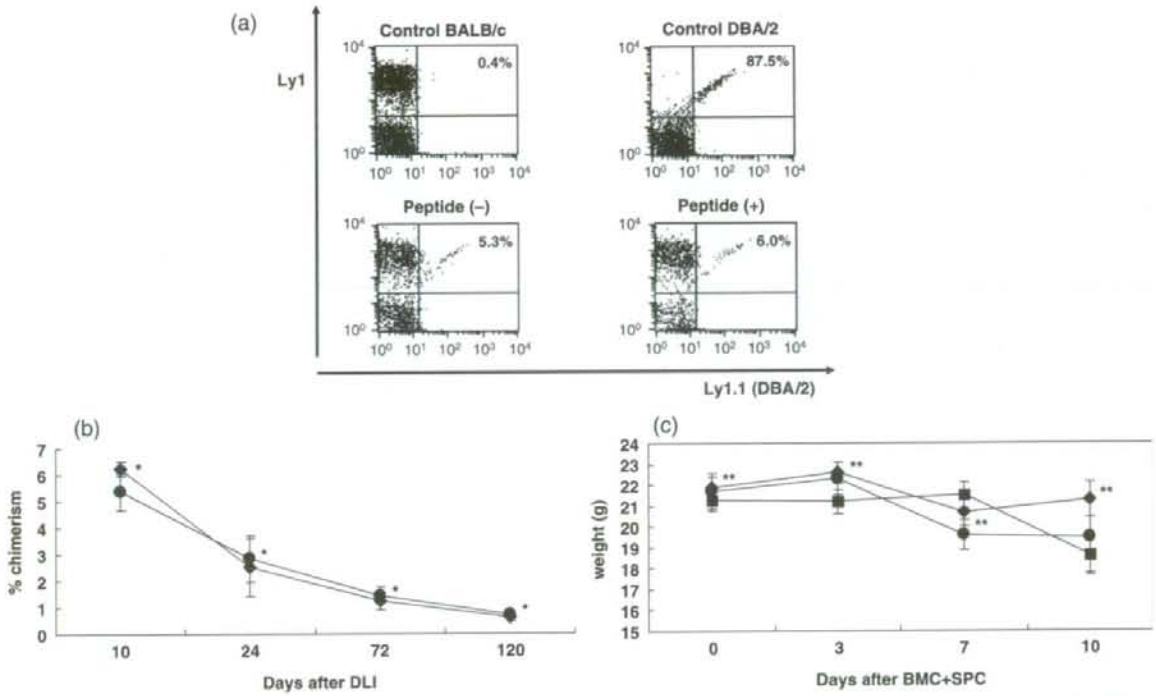

Fig. 3. Mixed chimerism and bodyweight in the BALB/c mice treated with the cyclophosphamide-utilizing cell therapy. (a) After establishing the injected tumors (usually 7 days after tumor inoculation), BALB/c mice were treated with spleen cells and bone marrow cells from DBA/2 mice on day 0 and cyclophosphamide on day 2, and donor lymphocytes infusion (DLI) from naive (Peptide [–]) or AH1 peptide-immunized BALB/c mice (Peptide [+]) on day 3. Ten days after the DLI, chimerism was assessed in each group by a flow cytometric analysis of the donor (Ly-1.1$^+$) cells in the peripheral blood. As a positive and a negative control, peripheral blood cells from untreated BALB/c (control BALB/c), untreated DBA/2 (control DBA/2) mice were examined. The representative experiment among three separate experiments is shown here. (b) Kinetic changes of donor chimerism are shown. After establishing the injected tumors (usually 7 days after tumor inoculation), BALB/c mice were treated with spleen cells and bone marrow cells from DBA/2 mice on day 0 and cyclophosphamide on day 2, and DLI from naive (●) or AH1 peptide-immunized (◆) BALB/c mice on day 3. The data represent the mean of three mice examined ± standard deviation (SD). The representative findings among three separate experiments are shown here. The other two experiments showed similar results. *P = NS. (c) Kinetic changes of bodyweight are shown. Symbols are same as (b). (■) Untreated control. The data represent the mean of five mice examined ± SD. **P = NS.

stimulated cells showed a high level of cytolytic activity against colon 26, but not P815. A similar result was observed when the spleen cells were *in vitro* stimulated with inactivated colon 26 cells (data not shown). These results indicate that tumor-specific CTL were induced in the mice that rejected colon 26 with the cyclophosphamide-using cell therapy with the DLI from tumor peptide-immunized donors.

Discussion

Non-myeloablative allogeneic SCT is an option for the treatment of several types of tumors. Although both alloantigens and tumor antigens could be targeted in GVT effects, studies in experimental models and clinical observations clearly suggest that alloantigens are primary targets for GVT.[11,28,29] Therefore, the involvement of tumor-specific T-cell immunity seems to be essential to enhance GVT effect without exacerbation of GVHD. To this end, two different protocols could be proposed: donor immunization and recipient immunization with tumor-specific antigens. In mouse models of melanoma, immunization of mice receiving allogeneic BMT following myeloablative conditioning with granulocyte-macrophage colony-stimulating factor (GM-CSF) secreting, irradiated tumor cell vaccines could induce antigen-specific tumor activity only in the absence of GVHD because

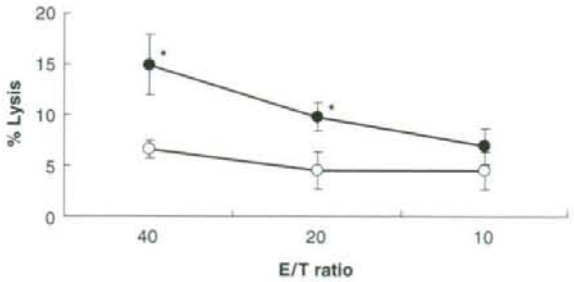

Fig. 4. Induction of colon 26-specific cytotoxic T lymphocytes from the cured BALB/c mice treated by the cyclophosphamide-using cell therapy with the donor lymphocytes infusion (DLI) from peptide-immunized donors. One hundred and twenty days after the DLI, spleen cells were removed from the colon 26-rejected BALB/c mice that had been treated by the cyclophosphamide-using cell therapy with the DLI from peptide-immunized donors, and were cultured *in vitro* with the AH1 peptide in the presence of interleukin (IL)-2 (50 U/mL) for 5 days. Thereafter, the cultured cells were examined for their cytolytic activity against either colon 26 (●) or P815 (○) tumor cells using a standard ^{51}Cr-release assay. *$P < 0.01$.

GVHD induces profound immunodeficiency.[30] Furthermore, it has been shown that DLI from tumor cell-immunized donors could induce tumor-specific antitumor immunity, again only in the absence of GVHD.[12] However, immunization of healthy donors with tumor cells, even though they are inactivated, hampers clinical application. In addition, immunization of donors with recipient-derived whole tumor cells potentially increases the risk of GVHD because the immunization induces the induction of antihost T-cell responses.[22] Taken together, immunization of donors with tumor antigen-derived peptides that have the potential to induce MHC class I-restricted cancer-reactive CTL could be an optimal strategy to produce tumor-specific T-cell immunity without causing GVHD. In fact, a number of CTL-inducing antigenic peptides have been identified so far,[25] and their safety in the clinical setting has been well verified. In the present study, we therefore searched for a possibility of non-myeloablative allogeneic SCT therapy in combination with the DLI from tumor peptide-immunized donors.

We recently proposed a unique model system of non-myeloablative allogeneic cell transplantation for the treatment of solid tumors by modifying our tolerance-inducing method using cyclophosphamide.[18,19] In this tolerance-inducing system, a stable degree of mixed chimerism as a result of the destruction of both donor-reactive T cells of host origin and host-reactive T cells of donor origin can be induced. By giving a donor lymphocytes from untreated donors 1 day after the cyclophosphamide treatment, the degree of mixed chimerism of donor cells increases in association with the development of transient mild GVHD, which is associated with antitumor effects in this model, probably because the DLI was carried out after the tolerance induction to donor cells.[20] In this study, we tested whether or not the DLI from either tumor cell-immunized or tumor peptide-immunized donors could augment non-myeloablative allogeneic cell therapy against s.c.-established colon 26 carcinoma. As a result, we revealed that the cyclophosphamide-using cell therapy with the DLI from tumor peptide-immunized donors could significantly augment antitumor effect.

An important observation of this study is that antitumor effect could be augmented by the DLI from tumor peptide-immunized donors without change of either donor chimerism or the degree of GVHD. In clinical allogeneic SCT, it is widely believed that the GVT activity is associated with GVHD and complete donor chimerism.[1,7,31,32] In this sense, it is a characteristic feature of the cyclophosphamide-using cell therapy that the antitumor activity is induced with low levels of donor chimerism.[20,21] Because the low levels of donor chimerism can reduce the risk of GVHD,[21,33,34] the cyclophosphamide-using cell therapy may be a choice of treatment especially for elderly patients or patients with a poor performance status or impaired organ functions. Indeed, similar post-transplant administration of cyclophosphamide has been recently applied to clinical non-myeloablative allogeneic SCT for hematological malignancies.[35,36] Taken together, the application of the DLI from tumor peptide-immunized donors seems to be optimal, because it could enhance the antitumor effects without hampering the merit of the cyclophosphamide-using cell therapy.

In this study, the immunization of DLI donors with a tumor antigen-derived AH1 peptide appears to be more effective to induce antitumor immunity than that with inactivated colon 26 carcinoma cells (Fig. 2a vs 2b, Table 1), although we did not directly compare the effects of the two strategies. This difference may be due to the difference in the methodology to immunize donors. First, a tumor peptide was given together with adjuvant, whereas inactivated colon 26 cells were i.p. injected into DBA/2 mice twice without adjuvant. Second, the route of vaccinations, s.c. versus i.p., was different. In addition, the immunization of healthy donors with carcinoma cells themselves, even though cells are inactivated, is ethically problematic and may potentially increase risk of GVHD.

Importantly, colon 26-cured mice that had been treated with the cyclophosphamide-using cell therapy with AH1-immunized donors showed cytolytic activity against colon 26 even after the disappearance of donor-derived lymphocytes, similar to our previous findings.[20,21] This means that the acquired immunity against colon 26 observed 120 days after DLI is considered to be mainly attributable to recipient lymphocytes. After the DLI from immunized donors, donor T cells encountering tumor antigens induce apoptosis of tumor cells and tumor-derived antigens may be engulfed by dendritic cells (DC) that present tumor antigens on their MHC molecules and further induce tumor-specific T cells of recipient origin. Interestingly, the antitumor response, despite loss of donor chimerism, has also been recently reported in patients treated with non-myeloablative conditioning and allogeneic SCT for advanced hematological malignancies.[37] In addition, both the critical role of recipient lymphocytes and the importance of recipient-derived γ-interferon in an antitumor effect have been recently reported in the mixed chimeras prepared with non-myeloablative conditioning in a murine model.[38] However, antitumor activity was induced by recipient lymphocyte infusion in their study,[38] but by DLI in our study.

Although the retroviral product may not reflect the real situation of antigens in human colon carcinoma, we utilized the peptide derived from the envelop protein of an endogenous murine leukemia virus[26] because the retroviral product is an endogenous, but not a foreign, antigen. The retrovirus is integrated in the genome of mice, and the gene product can be regarded as an endogenous antigen. In addition, several reports reveal that human endogenous retroviral products can be recognized by tumor-reactive CTL as tumor antigens in the cases of renal cell carcinoma and melanoma.[39,40] Therefore, retroviral products could be good target molecules in specific immunotherapy for a variety of malignancies.

In this study, we used CFA for peptide vaccination because peptide vaccination with incomplete Freund's adjuvant (IFA) in mice is insufficient to induce peptide-specific CTL *in vivo*.[41] On the other hand, in humans, peptide vaccination with IFA is enough to generate peptide-specific CTL in cancer patients.[42] For clinical trials, CFA is not essential in inducing peptide-specific CTL by vaccination with class I-binding peptides. We thus suppose that our protocol using IFA, in place of CFA, is applicable in a clinical setting.

doi: 10.1111/j.1349-7006.2008.01014.x

In conclusion, we demonstrate that the cyclophosphamide-using non-myeloablative cell therapy with DLI from tumor peptide-immunized donors can augment GVT effect without increasing the risk of GVHD. This strategy to strengthen antitumor activity without GVHD has important clinical implications.

Acknowledgments

This study was supported in part by a grant from the Ministry of Education, Science and Culture of Japan (no. 19591856) (to M. E.).

References

1 Childs R, Chernoff A, Contentin N *et al.* Regression of metastatic renal-cell carcinoma after nonmyeloablative allogeneic peripheral-blood stem-cell transplantation. *N Engl J Med* 2000; **343**: 750–8.

2 Slavin S, Nagler A, Naparstek E *et al.* Nonmyeloablative stem cell transplantation and cell therapy as an alternative to conventional bone marrow transplantation with lethal cytoreduction for the treatment of malignant and nonmalignant hematologic diseases. *Blood* 1998; **91**: 756–63.

3 Rini BI, Zimmerman T, Stadler WM, Gajewski TF, Vogelzang NJ. Allogeneic stem-cell transplantation of renal cell cancer after nonmyeloablative chemotherapy: feasibility, engraftment, and clinical results. *J Clin Oncol* 2002; **20**: 2017–24.

4 Pedrazzoli P, Da Prada GA, Giorgiani G *et al.* Allogeneic blood stem cell transplantation after a reduced-intensity, preparative regimen: a pilot study in patients with refractory malignancies. *Cancer* 2000; **94**: 2409–15.

5 Bregni M, Dodero A, Peccatori J *et al.* Nonmyeloablative conditioning followed by hematopoietic cell allografting and donor lymphocyte infusions for patients with metastatic renal and breast cancer. *Blood* 2002; **99**: 4234–6.

6 Hentschke P, Barkholt L, Uzunel M *et al.* Low-intensity conditioning and hematopoietic stem cell transplantation in patients with renal and colon carcinoma. *Bone Marrow Transplant* 2003; **31**: 253–61.

7 Ueno NT, Cheng YC, Rondón G *et al.* Rapid induction of complete donor chimerism by the use of a reduced-intensity conditioning regimen composed of fludarabine and melphalan in allogeneic stem cell transplantation for metastatic solid tumors. *Blood* 2003; **102**: 3829–36.

8 Bethge WA, Hegenbart U, Stuart MJ *et al.* Adoptive immunotherapy with donor lymphocyte infusions after allogeneic hematopoietic cell transplantation following nonmyeloablative conditioning. *Blood* 2004; **103**: 790–5.

9 Baron F, Baker JE, Storb R *et al.* Kinetics of engraftment in patients with hematologic malignancies given allogeneic hematopoietic cell transplantation after nonmyeloablative conditioning. *Blood* 2004; **104**: 2254–62.

10 Tykodi SS, Warren EH, Thompson JA *et al.* Allogeneic hematopoietic cell transplantation for metastatic renal cell carcinoma after nonmyeloablative conditioning: toxicity, clinical response, and immunological response to minor histocompatibility antigens. *Clin Cancer Res* 2004; **10**: 7799–811.

11 Horowitz MM, Gale RP, Sondel PM *et al.* Graft-versus-leukemia reactions after bone marrow transplantation. *Blood* 1990; **75**: 555–62.

12 Teshima T, Liu C, Lowler KP, Dranoff G, Ferrara JL. Donor leukocyte infusion from immunized donors increases tumor vaccine efficacy after allogeneic bone marrow transplantation. *Cancer Res* 2002; **62**: 796–800.

13 Martin PJ, Hansen JA, Buckner CD *et al.* Effects of in vitro depletion of T cells in HLA-identical allogeneic marrow grafts. *Blood* 1985; **66**: 664–72.

14 Kolb HJ, Mittermüller J, Clemm C *et al.* Donor leukocyte transfusions for treatment of recurrent chronic myelogenous leukemia in marrow transplant patients. *Blood* 1990; **76**: 2462–5.

15 Molldrem JJ, Lee PP, Wang C *et al.* Evidence that specific T lymphocytes may participate in the elimination of chronic myelogenous leukemia. *Nature Med* 2000; **6**: 1018–23.

16 Truitt RL, Johnson BD. Principles of graft-vs.-leukemia reactivity. *Biol Blood Marrow Transplant* 1995; **1**: 61–8.

17 Weiden PL, Flournoy N, Thomas ED *et al.* Antileukemic effect of graft-versus-host disease in human recipients of allogeneic-marrow grafts. *N Engl J Med* 1979; **300**: 1068–73.

18 Eto M, Mayumi H, Tomita Y, Yoshikai Y, Nomoto K. Intrathymic clonal deletion of V beta 6+ T cells in cyclophosphamide-induced tolerance to H-2-compatible, Mls-disparate antigens. *J Exp Med* 1990; **171**: 97–113.

19 Eto M, Mayumi H, Tomita Y *et al.* Specific destruction of host-reactive mature T cells of donor origin prevents graft-versus-host disease in cyclophosphamide-induced tolerant mice. *J Immunol* 1991; **146**: 1402–9.

20 Harano M, Eto M, Iwai T *et al.* Renal cancer treatment with low levels of mixed chimerism induced by nonmyeloablative regimen using cyclophosphamide in mice. *Cancer Res* 2005; **65**: 10032–40.

21 Eto M, Harano M, Tatsugami K *et al.* Cyclophosphamide-using nonmyeloablative allogenenic cell therapy against renal cancer with a reduced risk of graft-versus-host disease. *Clin Cancer Res* 2007; **13**: 1029–35.

22 Anderson LD Jr, Petropoulos D, Everse LA, Mullen CA. Enhancement of graft-versus-tumor activity and graft-versus-host disease by pretransplant immunization of allogenenic bone marrow donors with a recipient-derived tumor cell vaccine. *Cancer Res* 1999; **59**: 1525–30.

23 Anderson LD Jr, Mori S, Mann S, Savary CA, Mullen CA. Pretransplant tumor antigen-specific immunization of allogeneic bone marrow transplant donors enhances graft-versus-tumor activity without exacerbation of graft-versus-host disease. *Cancer Res* 2000; **60**: 5797–802.

24 Kwak LW, Taub DD, Duffey PL *et al.* Transfer of myeloma idiotype-specific immunity from an actively immunized marrow donor. *Lancet* 1995; **345**: 1016–20.

25 Novellino L, Castelli C, Parmiani G. A listing of human tumor antigens recognized by T cells: March 2004 update. *Cancer Immunol Immunother* 2005; **54**: 87–207.

26 Huang AY, Gulden PH, Woods AS *et al.* The immunodominant major histocompatibility complex class I-restricted antigen of a murine colon tumor derives from an endogenous retroviral gene product. *Proc Natl Acad Sci USA* 1996; **93**: 9730–5.

27 Eto M, Harada M, Tamada K *et al.* Antitumor activity of interleukin-12 against murine bladder cancer. *J Urol* 2000; **163**: 1549–52.

28 Reddy P, Maeda Y, Liu C, Krijanovski OI, Korngold R, Ferrara JL. A crucial role for antigen-presenting cells and alloantigen expression in graft-versus-leukemia responses. *Nature Med* 2005; **11**: 1244–9.

29 Matte CC, Liu J, Cormier J *et al.* Donor APCs are required for maximal GVHD but not for GVL. *Nature Med* 2004; **10**: 987–92.

30 Teshima T, Mach N, Hill GR, Gillessen PS, Dranoff G, Ferrara JL. Tumor cell vaccine elicits potent antitumor immunity after allogenic T-cell-depleted bone marrow transplantation. *Cancer Res* 2001; **61**: 162–71.

31 Huss R, Deeg HJ, Gooley T *et al.* Effect of mixed chimerism on graft-versus-host disease, disease recurrence and survival after HLA-identical marrow transplantation for aplastic anemia or chronic myelogenous leukemia. *Bone Marrow Transplant* 1996; **18**: 767–76.

32 Mattsson J, Uzunel M, Remberger M, Ringden O. T cell mixed chimerism is significantly correlated to a decreased risk of acute graft-versus-host disease after allogeneic stem cell transplantation. *Transplantation* 2001; **71**: 433–9.

33 Sykes M. Mixed chimerism and transplantation tolerance. *Immunity* 2001; **14**: 417–24.

34 Eto M, Kamiryo Y, Takeuchi A *et al.* Posttransplant administration of cyclophosphamide and donor lymphocyte infusion induces potent antitumor immunity to solid tumor. *Clin Cancer Res* 2008; **14**: 2833–40.

35 O'Donnell PV, Luznik L, Jones RJ *et al.* Nonmyeloablative bone marrow transplantation from partially HLA-mismatched related donors using posttransplantation cyclophosphamide. *Biol Blood Marrow Transplant* 2002; **8**: 377–86.

36 Luznik L, Fuchs EJ, Chen AR *et al.* Post-transplantation high-dose cyclophosphamide is effective single agent GVHD prophylaxis that permits prompt immune reconstitution after myeloablative HLA matched related and unrelated bone marrow transplantation. *Biol Blood Marrow Transplant Suppl* 2007; **13**: 4.

37 Dey BR, McAfee S, Colby C *et al.* Anti-tumour response despite loss of donor chimaerism in patients treated with non-myeloablative conditioning and allogeneic stem cell transplantation. *Br J Haematol* 2005; **128**: 351–9.

38 Rubio MT, Kim YM, Sachs T, Mapara M, Zhao G, Sykes M. Antitumor effect of donor marrow graft rejection induced by recipient leukocyte infusions in mixed chimeras prepared with nonmyeloablative conditioning: critical role for recipient-derived IFN-γ. *Blood* 2003; **102**: 2300–7.

39 Schiavetti F, Thonnard J, Colau D, Boon T, Coulie PG. A human endogenous retroviral sequence encoding an antigen recognized on melanoma by cytotoxic T lymphocytes. *Cancer Res* 2002; **62**: 5510–16.

40 Takahashi Y, Harashima N, Kajigaya S *et al.* Regression of human kidney cancer following allogeneic stem cell transplantation is associated with recognition of an HERV-E antigen by T cells. *J Clin Invest* 2008; **118**: 1099–109.

41 Bijker MS, van den Eeden SJF, Franken KL, Melief CJM, Offringa R, van der Burg SH. CD8+ CTL priming by exact peptide epitopes in incomplete Freund's adjuvant induces a vanishing CTL response, whereas long peptides induce sustained CTL reactivity. *J Immunol* 2007; **179**: 5033–40.

42 Rosenberg SA, Yang JC, Schwartzentruber DJ *et al.* Immunological and therapeutic evaluation of a synthetic peptide vaccine for the treatment of patients with metastatic melanoma. *Nature Med* 1998; **4**: 321–7.

Available online at www.sciencedirect.com
ScienceDirect
IJBCB
The International Journal of Biochemistry & Cell Biology 40 (2008) 598–603
www.elsevier.com/locate/biocel

Signalling networks in focus

Ku, Artemis, and ataxia-telangiectasia-mutated: Signalling networks in DNA damage

Tomohiro Morio [a,1,2], Hyeyoung Kim [b,*,1]

[a] *Department of Pediatrics and Developmental Biology, Tokyo Medical and Dental University, Graduate School of Medicine, Tokyo 113-8519, Japan*
[b] *Department of Food and Nutrition, Brain Korea 21 Project, College of Human Ecology, Yonsei University, Seoul 120-749, Republic of Korea*

Received 15 September 2007; received in revised form 6 December 2007; accepted 17 December 2007
Available online 24 December 2007

Abstract

Cell death linked to DNA damage has been implicated in various diseases caused by environmental stress and infection. Severe DNA damage, which is beyond the capacity of the DNA repair proteins, triggers apoptosis. Accumulation of DNA damage has been proposed to be a principal mechanism of infection, inflammation, cancer, and aging. The most deleterious form of DNA damage is double-strand breaks (DSBs), where ataxia-telangiectasia-mutated (ATM) is the main transducer of the double-strand DNA break signal. Once the DNA is damaged, the DNA repair protein Ku70/80 translocates into the nucleus, a process which may be mediated by ataxia-telangiectasia-mutated, a member of the phosphoinositide-3-kinase-like family. The function and stability of Artemis may also be regulated by ataxia-telangiectasia-mutated through its phosphorylation upon the occurrence of DNA damage. Interestingly, both Artemis and Ku70/80 are substrates of DNA-dependent protein kinase (DNA-PK), another member of the phosphoinositide-3-kinase-like family. In this review, we show how Ku and Artemis function in the DNA damage response and the ataxia-telangiectasia-mutated signaling pathway and discuss potential applications of agents targeting these DNA damage response molecules in the treatment of inflammation and cancer.

Keywords: Ku; Artemis; Ataxia-telangiectasia-mutated; DNA damage

Abbreviations: AT, ataxia-telangiectasia; ATM, ataxia-telangiectasia-mutated; ATR, ataxia-telangiectasia and Rad3-related; DNA-PK, DNA-dependent protein kinase; DNA-PKcs, catalytic subunit of DNA-dependent protein kinase; DSBs, double-strand breaks; ROS, reactive oxygen species; NHEJ, non-homologous end joining; HR, homologous recombination; PI-3-kinase, phosphoinositide-3-kinase; CHK2, checkpoint 2 kinase; CdK, cyclin-dependent kinase; M/R/N complex, Mre11/Rad50/NBS1; ATRIP, ATR-interacting protein; XRCC4, X-ray repair complementing defective repair in Chinese hamster cells 4; Mre11, meiotic recombination 11; NBS1, Nijmegen breakage syndrome 1; MDM2, mouse double minute 2; H2AX, histone H2AX; IgCS, immunoglobulin class switch.

* Corresponding author. Tel.: +82 2 2123 3125; fax: +82 2 364 5781.
E-mail addresses: tmorio.ped@tmd.ac.jp (T. Morio), kim626@yonsei.ac.kr (H. Kim).
[1] Both the authors contributed equally to the work.
[2] Tel.: +81 3 5803 5245; fax: +81 3 5803 5245.

1357-2725/$ – see front matter © 2007 Elsevier Ltd. All rights reserved.
doi:10.1016/j.biocel.2007.12.007

Signaling network facts

- Ataxia-telangiectasia-mutated, Ku70/80, and Artemis are involved in the cellular pathways that work to repair DNA double-strand breaks.
- Ku70/80 and Artemis play a crucial role in non-homologous end joining by interacting with other molecules, such as X-ray repair complementing defective repair in Chinese hamster cells 4 (XRCC4), DNA ligase IV, and Cernunnos. Ataxia-telangiectasia-mutated plays a mediating role in homologous recombinational repair of DNA damage by interacting with meiotic recombination 11/Rad50/Nijmegen breakage syndrome 1.
- Functions of Ku70/80 and Artemis are, at least in part, controlled by phosphorylation by DNA-dependent protein kinase. Ku70/80 and Artemis are also substrates of ataxia-telangiectasia-mutated.
- The ataxia-telangiectasia-mutated signal is critical in cell cycle control and in cellular apoptosis via the p53 pathway.
- Ku proteins translocate into the nucleus upon the occurrence of DNA damage, and their nuclear transports are possibly controlled by phosphorylation.
- Nuclear loss of Ku proteins or ataxia-telangiectasia-mutated may be the underlying mechanism of oxidative stress-induced apoptotic cell death.

1. Introduction

Many types of DNA damage can occur within cells, but the most dangerous are double-strand breaks (DSBs). These results from exogenous agents (such as ionizing radiation, chemotherapeutic drugs, and infectious agents), endogenously generated reactive oxygen species (ROS), and mechanical stress acting on the chromosomes. DSBs can also be produced when DNA replication forks encounter DNA single-strand breaks or other lesions. Accumulation of DNA damage, leading to adult stem cell exhaustion, has been proposed as a principal mechanism of aging (Nijnik et al., 2007).

DNA repair proteins, such as DNA-dependent protein kinase (DNA-PK), Ku, and ataxia-telangiectasia-mutated (ATM), have been linked to cellular DNA repair pathways that work to fix DNA DSBs, while ataxia-telangiectasia and Rad3-related (ATR) is activated by many forms of DNA damage. Ku70/80 and Artemis are involved in non-homologous end joining (NHEJ) by interacting with other molecules, such as X-ray repair complementing defective repair in Chinese hamster cells 4 (XRCC4), DNA ligase IV, and Cernunnos. ATM is involved in homologous recombinational repair of DNA damage by interaction with meiotic recombination 11 (Mre11)/Rad50/Nijmegen breakage syndrome 1 (NBS1) (M/R/N complex), cell cycle arrest by the phosphorylation of various molecules such as checkpoint 2 kinase (CHK2), and cellular apoptosis via the p53 pathway.

ATM and DNA-PK may regulate the function of Ku70/80 and Artemis by phosphorylation and/or nuclear transport of Ku proteins and Artemis. In oxidative stress-induced DNA damage, ATM is essential for Ku activation and cell survival. The nuclear loss of Ku 70/80 or ATM is observed upon genotoxic stimuli. Degradation of these molecules may be another underlying mechanism of apoptosis. Further studies on the regulatory mechanisms and signaling networks of DNA damage response molecules are needed to better understand the complex cellular response. This review focuses on the interplay among ATM, Artemis, and Ku70/80 in response to DNA DSBs.

2. Key molecules and functions

2.1. Ku70/80 and DNA damage

The Ku70 (70 kDa) and Ku80 (80 kDa) proteins are DNA-binding regulatory subunits of DNA-PK, which is composed of a 470 kDa catalytic subunit (DNA-PKcs) and Ku proteins. Ku70 and Ku80 initiate the repair process of DNA DSBs, which produce DNA fragmentation, by activating DNA-PK after binding to the DNA DSBs. In addition to the regulatory function of the Ku proteins in DNA-PK, heterodimers of Ku70 and Ku80 have independent DNA repair functions. These include single-stranded DNA-dependent ATPase activity and the binding and repair of broken single-stranded DNA, single-stranded nicks, gaps in DNA, and single-strand-to-double-strand transitions in DNA. The importance of Ku70/80 in DSBs is highlighted by the fact that Ku70-deficient cells have increased ionizing radiosensitivity, defective DNA end-binding activity, and impaired V(D)J recombination. Ku80-null mice display an increase in chromosomal aberrations and malignant transformation

(Difilippantonio et al., 2000; Gu, Jin, Gao, Weaver, & Alt, 1997).

Ku70/80 plays a critical role in the repair of damaged DNA through NHEJ by interacting with XRCC4, Cernunnos, and DNA ligase IV. Phosphorylation of Ku70/80 by DNA-PK controls their localization, DNA binding, and function. DNA-PK phosphorylates Artemis, p53, and histone H2AX, which determine the fate of the cells.

Oxidative stress can be caused by ionizing radiation, cytotoxic drugs, infection, inflammation, cancer, and aging. It leads to the generation of single-strand breaks and DSBs. Oxidative stress-induced DNA damage of haematopoietic stem cells during aging is repaired mainly by NHEJ, in which Ku70/80 has a critical role, but ATM may also be involved (Nijnik et al., 2007). Oxidative injury caused by mild ischemia/reperfusion in the spinal cord induces reversible neurological deficits with increased Ku-DNA binding activity, whereas severe ischemia/reperfusion causes permanent deficits that are accompanied by a decrease in the Ku-DNA binding activity. Therefore, Ku may have a protective role against oxidative injury (Shackelford, Tobaru, Zhang, & Zivin, 1999). Embryonic fibroblasts derived from Ku80-null mice are more susceptible to DNA damage than those from wild-type mice (Arrington et al., 2000), suggesting that a decrease in Ku may be involved in the mechanism of apoptotic cell death. DNA-PKcs is the substrate for caspase-3, which is activated by ischemia/reperfusion and ROS. The reduction in Ku might be induced in a caspase-activating apoptotic pathway after ischemia/reperfusion (Shackelford et al., 1999). Nuclear localization of Ku70 and Ku80 are mediated by two compartments of the nuclear pore-targeting complex, importin α and importin β. Oxidative stress-induced apoptosis is mediated by the activated caspase-3, which degrades Ku70/80 (Song, Lim, Kim, Morio, & Kim, 2003). A decrease in Ku binding to nuclear transporters importin α and importin β results in reduced levels of nuclear Ku70/80 in pancreatic acinar cells. Further studies are required to determine the mechanism of selective reduction of each Ku component upon the occurrence of DNA damage in the cells.

2.2. *Ku70/80 as a signaling molecule*

Ku70/80 are located in the cytoplasm and on the cell surface (Morio et al., 1999). Ku70 serves as a receptor for *Rickettsia conorii* internalization (Martinez, Seveau, Veiga, Matsuyama, & Cossart, 2005). Ku70/80 is associated with CD40 in the cytoplasm, and CD40 engagement leads to the translocation of Ku70/80 to the cell surface of multiple myeloma cells. In normal human B cells, Ku70/80 resides in the cytoplasm and translocates to the nucleus upon the receipt of the immunoglobulin class switch (IgCS)-inducing signal or upon DNA damage. Since B cells need NHEJ mediated by Ku70/80 when they undergo IgCS (Morio et al., 1999), Ku70/80 may act as a signaling molecule in this cellular process.

Modification of Ku70 and Ku80 takes place when DNA is damaged, and the functional consequences of this modification are of particular interest. Polyglutamine (polyQ) diseases, such as Huntington's disease and Machado-Joseph disease, are caused by the gain of a toxic function by abnormally expanded polyQ tracts. An expanded polyQ of ataxin-3, a gene that causes Machado-Joseph disease, stimulates Ku70 acetylation. This post-translational modification of Ku70 dissociates the proapoptotic protein Bax from Ku70, thereby promoting Bax activation and subsequent cell death. This suggests that cell death is, at least in part, controlled by acetylation of Ku70 (Li et al., 2007). The physiological relevance of Ku phosphorylation is still an enigma. There are four DNA-PK phosphorylation sites on the Ku70/80 heterodimer: serine 6 of Ku70, serine 577 and 580 and threonine 715 of Ku80. However, neither DNA-PK nor ATM is required for phosphorylation of these sites on the Ku70/80 heterodimer *in vivo*. DNA-PK-dependent phosphorylation of Ku70/80 is not required for NHEJ either. The involvement of ATM in Ku70/80 modification awaits further study.

2.3. *ATM and Ku70/80*

ATM is the protein product of the gene mutated in the multisystem disorder ataxia-telangiectasia (AT), which is characterized by neuronal degeneration, immunodeficiency, chromosomal instability, and a predisposition to cancer formation. ATM is a large molecule with serine/threonine kinase activity, and it functions in DNA damage responses and cell cycle control. DSB recognition is the first step in the DSB damage response and involves activation of ATM and phosphorylation of targets, such as p53, to trigger cell cycle arrest, DNA repair, or apoptosis. The activation of ATR kinase by DSBs also occurs in an ATM-dependent manner. On the other hand, Ku70/80 is known to participate at a later time in the DSB response, recruiting DNA-PKcs to facilitate NHEJ. Recent finding shows that Ku70/80 plays a novel role in modulating ATM-dependent ATR activation during the DSB damage response and confers a protective effect against ATM-independent ATR activation at later stages of the DSB damage response (Tomimatsu et al., 2007). Following exposure to genotoxic stress, proliferating cells actively slow down DNA

replication through an S phase checkpoint to provide time for repair. The ATM-dependent pathway plays an important role in the S phase checkpoint response following ionizing radiation. Stronger S checkpoint activity in irradiated Ku80-null cells is due to the higher ATM kinase activity. Ku affects the ATM-dependent S phase checkpoint following ionizing radiation (Zhou et al., 2002). Ionizing radiation exposure results in the upregulation of Ku70 via a p53/ATM-dependent mechanism. Increased oxidative stress has been reported in neuronal tissues of ATM-deficient mice (Kamsler, Daily, Hochman, Stern, & Shiloh, 2001). It is not clear whether ATM itself is directly involved in sensing the increase in ROS or whether oxidative stress in AT cells is associated with unrepaired DSBs continuously present in the DNA. Transfecting AT cells with the full-length ATM gene assures cell death prevention, which may be assisted by the activation of Ku in response to oxidative stress (Lee, Kim, Morio, & Kim, 2006). ATM may be essential for Ku activation in the process of repairing DNA damage and preventing cell death.

2.4. ATM and Artemis

Artemis was originally identified as deficient in human radiosensitive severe combined immunodeficiency syndrome. Artemis exhibits an intrinsic single strand-specific 5′ to 3′ exonuclease activity and has hairpin-opening endonuclease activity, which is induced by phosphorylation by DNA-PK. Artemis has roles in V(D)J recombination, NHEJ, and regulation of the DNA damage-induced G2/M cell cycle checkpoint. Cells with mutations in the Artemis gene and Artemis-deficient cells exhibit radiosensitivity and defective V(D)J recombination, implicating the Artemis function in NHEJ (Wang et al., 2005). Since the NHEJ reaction functions as a genomic caretaker, particularly in the prevention of translocations and telomere fusions, Artemis deficiency may be related to carcinogenesis.

The *bona fide* phosphorylation sites and physiological relevance of the phosphorylation are, however, still under investigation. Three basic phosphorylation sites (S385, S516/518) and 11 DNA-PK phosphorylation sites were identified by proteomic analysis using matrix-assisted laser desorption/ionization-time of flight mass spectrometry (MALDI-TOF MS). There were nine other putative DNA-PK/ATM phosphorylation sites identified. Most of the phosphorylation sites are clustered in the C-terminus region. It is now evident that Artemis is a downstream component of the ATM signaling pathway; ATM is the major kinase responsible for the modification of Artemis (Poinsignon et al., 2004; Riballo et al., 2004; Zhang et al., 2004). One of the target sites of ATM is S645 of Artemis, and its phosphorylation leads to hyperphosphorylation of Artemis. Artemis phosphorylation by ATM is important in association with the M/R/N complex and Cdk1-cyclin B activation, which in turn controls G2/M checkpoint recovery. On the other hand, phosphatase-treated mammalian Artemis still retains endonuclease activity. Artemis molecule lacking the C-terminal domain is sufficient to complement V(D)J recombination in Artemis-null cells. How endonuclease activity of Artemis and its association with the damaged termini are controlled is still controversial. DNA-PK, ATM, and other not-yet-identified kinase(s) could be involved in the pathway leading to Artemis activation.

3. Cascades

As for DSBs, ATM phosphorylates key proteins in the salvage pathways leading to DSB repair and activation of cell cycle checkpoints (Fig. 1). DNA repair proteins interact with other molecules to repair the damaged DNA through NHEJ or homologous recombination (HR). For instance, ATM phosphorylates key proteins (Ku70/80 and Artemis) to repair the damaged DNA by NHEJ. On the other hand, ATM temporarily arrests the cell cycle by phosphorylating CHK2, which in turn phosphorylates p53, while the damage is being repaired. ATM repairs the damaged DNA through HR by interacting with ATR and the M/R/N complex. When the attempt to repair the

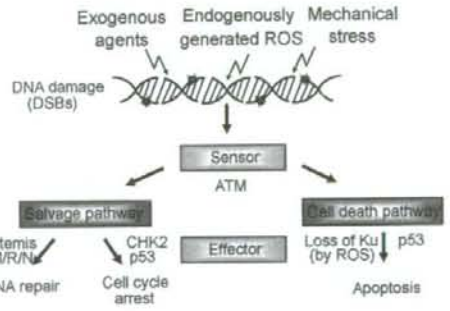

Fig. 1. Cell responses to DNA damage. Upon the formation of DSBs, ATM serves as a sensor for DNA damage and phosphorylates key proteins in pathways leading to DSB repair or the activation of cell cycle checkpoints. ATM phosphorylates key proteins (Ku70/80, Artemis) to repair the damaged DNA. Additionally, ATM temporarily arrests the cell cycle by phosphorylating CHK2, which in turn phosphorylates p53, while the damage is being repaired. ATM repairs the damaged DNA through HR by interacting with ATR and the M/R/N complex. When the attempt to repair the damage fails, the cell undergoes apoptosis via the p53 pathway. Oxidative stress-induced cell death stems from the nuclear loss of Ku70/80.

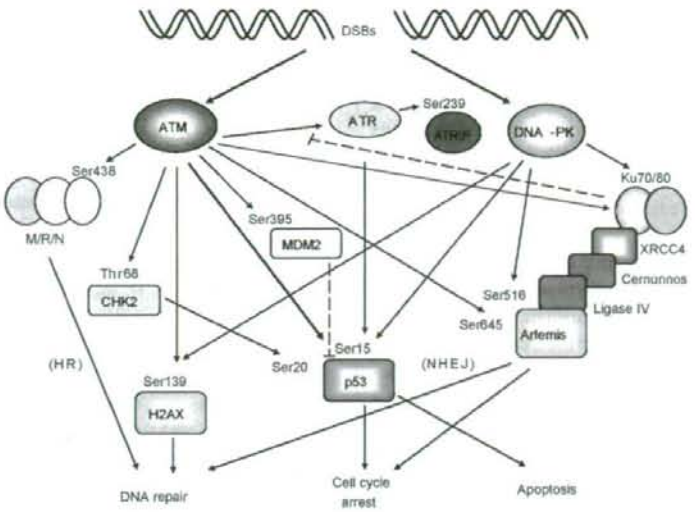

Fig. 2. Targets for the ATM/DNA-PK phosphorylation and signaling network. DNA-PK, ATM, and ATR are recruited to the sites of DNA damage through analogous mechanisms involving conserved interaction motifs observed in Ku80, NBS1, and ATRIP, respectively. Ku70/80 and Artemis play critical roles in the repair of damaged DNA through NHEJ by interacting with XRCC4/Cernunnos/DNA ligase IV. Phosphorylation of Ku70/80 and Artemis by DNA-PK and ATM controls cell cycle arrest and the DNA repair function. ATM triggers the repair of damaged DNA through HR by interacting with the M/R/N complex. ATM phosphorylates CHK2, which phosphorylates p53 to arrest the cell cycle, while damage is being repaired. When the attempt to repair the damage fails, the cell undergoes apoptosis via the p53 pathway. Dotted lines: Ku70/80 also affects ATM-dependent ATR activation. The stability of p53 is also tightly controlled by MDM2.

damage fails, the cell undergoes apoptosis via the p53 pathway. Oxidative stress-induced cell death stems from the nuclear loss of Ku70/80 (Song et al., 2003).

As shown in Fig. 2, DNA repair is mediated by DNA damage response molecules and involves three members of the phosphoinositide-3-kinase-like family (ATM, ATR, and DNA-PK). DNA-PK, ATM, and ATR are recruited to the sites of DNA damage through analogous mechanisms involving conserved interaction motifs observed in Ku80, NBS1, and ATRIP, respectively. The DNA-PK/Ku70/80 complex is required for the NHEJ DNA repair pathway. Artemis plays a role in processing the DNA ends prior to ligation. XRCC4/Cernunnos/DNA ligase IV is recruited to the DNA-PK/Ku complex, which is required for end joining. ATM plays a role in DNA DSB repair in concert with the M/R/N complex. DNA-PK and ATM share several substrates as phosphorylation targets, including Artemis, p53, and histone H2AX. Interplays among Ku70/80, Artemis, DNA-PK, and ATM are involved in DNA damage responses. Ku70/80 also affects ATM-dependent ATR activation. Degradation of key signaling molecules (p53, Ku70/80, and Artemis) is one of the mechanisms determining cell fate. Oxidative stress-induced degradation of Ku70/80 is mediated by caspase-3 (Song et al., 2003). Activity of p53 is regulated by the ubiquitin–proteasome system, which is the major non-lysosymal system for degrading proteins in the cell (Thompson et al., 2007). It is still unclear whether Ku70/80 and Artemis are similarly regulated by proteasome-dependent degradation or other protease systems. Degradation of Ku70/80 leads to upregulation of p53, resulting in apoptosis. The stability of p53 is also tightly controlled by mouse double minute 2 (MDM2) (Fig. 2).

4. Associated pathologies and therapeutic implications

Nuclear loss of Ku70/80 and DNA damage linked to oxidative stress in pancreatic acinar cells has been suggested as pathophysiologic mechanisms of pancreatitis (Song et al., 2003). DNA-PK deficiency in cultured neurons causes an accumulation of DNA damage and increased susceptibility to apoptosis (Chechlacz, Vemuri, & Naegele, 2001). Diminished DNA DSB repair by NHEJ causes a progressive loss of haematopoietic stem cells and bone marrow cellularity during aging (Nijnik et al., 2007). Therefore, the loss of function of Ku proteins and DNA-PK activity might be one of

the important pathological mechanisms in apoptotic cell death related to pancreatic inflammation, neurological disorders, and aging. Since ATM is essential for nuclear Ku activation, maintenance of Ku70/80 and DNA-PK together with ATM may prevent DNA damage in various diseases and inflammation. Artemis serves as a tumor suppressor and patients with hypomorphic mutations in Artemis have a predisposition to develop lymphoma (Moshous et al., 2003). Phosphorylation and degradation of Artemis may be a key step in controlling cellular apoptosis and carcinogenesis. The formation of carcinogenic translocations requires the illegitimate joining of chromosomes containing DSBs. The molecules presented in this review are critical in DNA repair, and their defective function, improper localization, and loss may lead to unrepaired DNA DSBs and to the malignant transformation of cells when they escape apoptosis. The manipulation of these DNA damage response molecules could lead to anti-inflammatory agents and anti-cancer agents.

Acknowledgements

This study was supported by a grant (Joint Research Project under the Korea-Japan Basic Scientific Cooperation Program) from the Korea Science and Engineering Foundation (F01-2006-000-10063-0) (to H. Kim) and from JSPS (to T. Morio). H. Kim is grateful to the Brain Korea 21 Project, Yonsei University.

References

Arrington, E. D., Caldwell, M. C., Kumaravel, T. S., Lohani, A., Joshi, A., Evans, M. K., et al. (2000). Enhanced sensitivity and long-term G2 arrest in hydrogen peroxide-treated Ku80-null cells are unrelated to DNA repair defects. *Free Rad. Biol. Med., 29*, 1166–1176.

Chechlacz, M., Vemuri, M. C., & Naegele, J. R. (2001). Role of DNA-dependent protein kinase in neuronal survival. *J. Neurochem., 78*, 141–154.

Difilippantonio, M. J., Zhu, J., Chen, H. T., Meffre, E., Nussenzweig, M. C., Max, E. E., et al. (2000). DNA repair protein Ku80 suppresses chromosomal aberrations and malignant transformation. *Nature, 404*, 823–825.

Gu, Y., Jin, S., Gao, Y., Weaver, D. T., & Alt, F. W. (1997). Ku70-deficient embryonic stem cells have increased ionizing radiosensitivity, defective DNA end-binding activity, and inability to support V(D)J recombination. *Proc. Natl. Acad. Sci. U.S.A., 94*, 8076–8081.

Kamsler, A., Daily, D., Hochman, A., Stern, N., & Shiloh, Y. (2001). Increased oxidative stress in ataxia telangiectasia evidenced by alterations in redox state of brains from Atm-deficient mice. *Cancer Res., 61*, 1849–1854.

Lee, J. H., Kim, K. H., Morio, T., & Kim, H. (2006). Ataxia-telangiectasia-mutated-dependent activation of Ku in human fibroblasts exposed to hydrogen peroxide. *Ann. N.Y. Acad. Sci., 1090*, 542–548.

Li, Y., Yokota, T., Gama, V., Yoshida, T., Gomez, J. A., Ishikawa, K., et al. (2007). Bax-inhibiting peptide protects cells from polyglutamine toxicity caused by Ku70 acetylation. *Cell Death Differ., 14*, 2058–2067.

Martinez, J. J., Seveau, S., Veiga, E., Matsuyama, S., & Cossart, P. (2005). Ku70, a component of DNA-dependent protein kinase, is a mammalian receptor for *Rickettsia conorii*. *Cell, 12*, 1013–1023.

Morio, T., Hanissian, S. H., Bacharier, L. B., Teraoka, H., Nonoyama, S., Seki, M., et al. (1999). Ku in the cytoplasm associates with CD40 in human B cells and translocates into the nucleus following incubation with IL-4 and anti-CD40 mAb. *Immunity, 11*, 339–348.

Moshous, D., Pannetier, C., Chasseval, R. R., Deist, F. F., Cavazzana-Calvo, M., Romana, S., et al. (2003). Partial T and B lymphocyte immunodeficiency and predisposition to lymphoma in patients with hypomorphic mutations in Artemis. *J. Clin. Invest., 111*, 381–387.

Nijnik, A., Woodbine, L., Marchetti, C., Dawson, S., Lambe, T., Liu, C., et al. (2007). DNArepair is limiting for haematopoietic stem cells during ageing. *Nature, 447*(7145), 686–690.

Poinsignon, C., de Chasseval, R., Soubeyrand, S., Moshous, D., Fischer, A., Hache, R. J., & de Villartay, J. P. (2004). Phosphorylation of Artemis following irradiation-induced DNA damage. *Eur. J. Immunol., 34*, 3146–3155.

Riballo, E., Kuhne, M., Rief, N., Doherty, A., Smith, G. C., Recio, M. J., et al. (2004). A pathway of double-strand break rejoining dependent upon ATM, Artemis, and proteins locating to gamma-H2AX foci. *Mol. Cell, 16*, 715–724.

Shackelford, D. A., Tobaru, T., Zhang, S., & Zivin, J. A. (1999). Changes in expression of the DNA repair protein complex DNA-dependent protein kinase after ischemia and reperfusion. *J. Neurosci., 19*, 4727–4738.

Song, J. Y., Lim, J. W., Kim, H., Morio, T., & Kim, K. H. (2003). Oxidative stress induces nuclear loss of DNA repair proteins, Ku70 and Ku80, and apoptosis in pancreatic acinar AR42J cells. *J. Biol. Chem., 278*, 36676–36687.

Thompson, S. J., Loftus, L. T., Ashley, M. D., & Meller, R. (2007). Ubiquitin–proteasome system as a modulator of cell fate. *Curr Opin Pharmacol.*, on-line publication [Epub ahead of print].

Tomimatsu, N., Tahimic, C. G., Otsuki, A., Burma, S., Fukuhara, A., Sato, K., et al. (2007). Ku70/80 modulates ATM and ATR signaling pathways in response to DNA double strand breaks. *J. Biol. Chem., 282*, 10138–10145.

Wang, J., Pluth, J. M., Cooper, P. K., Cowan, M. J., Chen, D. J., & Yannone, S. M. (2005). Artemis deficiency confers a DNA double-strand break repair defect and Artemis phosphorylation status is altered by DNA damage and cell cycle progression. *DNA Repair (Amst), 4*(5), 556–570.

Zhang, X., Succi, J., Feng, Z., Prithivirajsingh, S., Stpry, M. D., & Legerski, R. J. (2004). Artemis is a phosphorylation target of ATM and ATR and is involved in the G2/M DNA damage checkpoint response. *Mol. Cell Biol., 24*, 9207–9220.

Zhou, X. Y., Wang, X., Wang, H., Chen, D. J., Li, G. C., Iliakis, G., & Wang, Y. (2002). Ku affects the ATM-dependent S phase checkpoint following ionizing radiation. *Oncogene, 21*, 6377–6381.

Cell

Tyrosine Kinases Btk and Tec Regulate Osteoclast Differentiation by Linking RANK and ITAM Signals

Masahiro Shinohara,[1,2] Takako Koga,[1,2] Kazuo Okamoto,[1,2] Shinya Sakaguchi,[4] Kimiko Arai,[1,5] Hisataka Yasuda,[7] Toshiyuki Takai,[6] Tatsuhiko Kodama,[8] Tomohiro Morio,[3] Raif S. Geha,[9] Daisuke Kitamura,[10] Tomohiro Kurosaki,[11] Wilfried Ellmeier,[4] and Hiroshi Takayanagi[1,2,*]

[1]Department of Cell Signaling, Graduate School
[2]Center of Excellence Program for Frontier Research on Molecular Destruction and Reconstruction of Tooth and Bone
[3]Department of Pediatrics and Developmental Biology, Graduate School
Tokyo Medical and Dental University, Yushima 1-5-45, Bunkyo-ku, Tokyo 113-8549, Japan
[4]Institute of Immunology, Center for Physiology, Pathophysiology, and Immunology, Medical University of Vienna, Lazarettgasse 19, Vienna 1090, Austria
[5]Division of Orthodontics and Dentofacial Orthopedics, Graduate School of Dentistry
[6]Department of Experimental Immunology, Institute of Development, Aging, and Cancer
Tohoku University, Seiryo-machi 4-1, Aoba-ku, Sendai, Miyagi 980-8575, Japan
[7]Nagahama Institute for Biochemical Science, Oriental Yeast Co., Ltd., Kanoh-cho 50, Nagahama, Shiga 526-0804, Japan
[8]Department of Molecular Biology and Medicine, Research Center for Advanced Science and Technology, University of Tokyo, Komaba 4-6-1, Meguro-ku, Tokyo 153-8904, Japan
[9]Division of Immunology, Children's Hospital, One Blackfin Circle, Boston, MA 02115, USA
[10]Division of Molecular Biology, Research Institute for Biological Sciences, Tokyo University of Science, Yamazaki 2669, Noda, Chiba 278-0022, Japan
[11]Laboratory for Lymphocyte Differentiation, RIKEN Research Center for Allergy and Immunology, RIKEN Yokohama Institute, Suehiro-cho 1-7-22, Tsurumi-ku, Yokohama, Kanagawa 230-0045, Japan
*Correspondence: taka.csi@tmd.ac.jp
DOI 10.1016/j.cell.2007.12.037

SUMMARY

Certain autoimmune diseases result in abnormal bone homeostasis, but association of immunodeficiency with bone is poorly understood. Osteoclasts, which derive from bone marrow cells, are under the control of the immune system. Differentiation of osteoclasts is mainly regulated by signaling pathways activated by RANK and immune receptors linked to ITAM-harboring adaptors. However, it is unclear how the two signals merge to cooperate in osteoclast differentiation. Here we report that mice lacking the tyrosine kinases Btk and Tec show severe osteopetrosis caused by a defect in bone resorption. RANK and ITAM signaling results in formation of a Btk(Tec)/BLNK(SLP-76)-containing complex and PLCγ-mediated activation of an essential calcium signal. Furthermore, Tec kinase inhibition reduces osteoclastic bone resorption in models of osteoporosis and inflammation-induced bone destruction. Thus, this study reveals the importance of the osteoclastogenic signaling complex composed of tyrosine kinases, which may provide the molecular basis for a new therapeutic strategy.

INTRODUCTION

Bone homeostasis depends on balanced action of bone-resorbing osteoclasts and bone-forming osteoblasts (Karsenty and Wagner, 2002). Tipping the balance in favor of osteoclasts leads to diseases with a low bone mass, whereas impaired osteoclastic bone resorption results in diseases with a high bone mass, including osteopetrosis (Teitelbaum and Ross, 2003). Bone reserves calcium and responds to calcium-regulating hormones, but osteoclasts and osteoblasts are not only regulated by the endocrine system. The immune and bone systems share numerous regulatory factors, including cytokines, receptors, signaling molecules, and transcription factors (Theill et al., 2002; Walsh et al., 2006; Takayanagi, 2007). Therefore, the pathology of one system may very well affect the other: it is well documented that enhanced bone resorption is associated with activation of the immune system observed in autoimmune or inflammatory diseases such as rheumatoid arthritis and periodontitis (Theill et al., 2002; Takayanagi, 2007).

Diseases with impaired immune responses are also associated with bone abnormalities, but it is poorly understood how the immunodeficiencies are functionally related to bone disorders. Hyperimmunoglobulin E (IgE) syndrome is characterized by skeletal symptoms such as osteoporosis (Kirchner et al., 1985) and scoliosis (Grimbacher et al., 1999), which are partly explained by the abnormality of osteoblasts and osteoclasts

caused by the mutation in the *STAT3* gene. (Minegishi et al., 2007). X-linked hyper-IgM syndrome (caused by a mutation in the *CD40L* gene) has a skeletal complication, osteopenia, which is attributed to enhanced osteoclast formation due to the impaired production of interferon-γ by T cells (Lopez-Granados et al., 2007). Thus, exploring the mechanisms underlying skeletal complications in primary immunodeficiencies will be important for understanding the shared mechanisms and crosstalk between immune and bone systems.

The osteoclast was the first skeletal cell to be determined to be under the control of the immune system (Horton et al., 1972). Because osteoclasts originate from bone marrow-derived monocyte/macrophage precursor cells (BMMs) of hematopoietic lineage, many regulators of osteoclast differentiation are also utilized in the control of the innate and adaptive immune systems. The differentiation of osteoclasts is mainly regulated by three signaling pathways activated by receptor activator of nuclear factor-κB ligand (RANKL), macrophage colony-stimulating factor (M-CSF), and immunoreceptor tyrosine-based activation motif (ITAM) (Asagiri and Takayanagi, 2007). Whereas M-CSF promotes the proliferation and survival of BMMs (Ross and Teitelbaum, 2005), RANKL activates the differentiation process by inducing the master transcription factor for osteoclastogenesis, nuclear factor of activated T cells c1 (NFATc1), via the tumor necrosis factor receptor-associated factor 6 (TRAF6) and c-Fos pathways (Takayanagi et al., 2002). The induction of NFATc1 is also dependent on the calcium signal, which is mediated by the activation of ITAM in adaptor molecules such as DNAX-activating protein 12 (DAP12) and Fc receptor common γ subunit (FcRγ) (Koga et al., 2004; Mocsai et al., 2004) in association with costimulatory receptors of the immunoglobulin superfamily, including triggering receptor expressed in myeloid cells-2 (TREM-2), signal-regulatory protein β1 (SIRPβ1), paired immunoglobulin-like receptor-A (PIR-A), and osteoclast-associated receptor (OSCAR) (Koga et al., 2004). Phosphorylation of ITAM results in recruitment of the nonreceptor tyrosine kinase Syk, leading to the activation of phospholipase Cγ (PLCγ) and calcium mobilization (Faccio et al., 2003; Koga et al., 2004; Mocsai et al., 2004; Mao et al., 2006), but osteoclastogenesis cannot be induced by costimulatory signals alone and requires RANKL stimulation. However, it has been unclear how RANK and ITAM signals merge to cooperatively stimulate the downstream signaling pathway.

To identify the molecules activated by RANKL that stimulate the calcium signaling pathway by functioning as an integrator of the RANK and ITAM signals, we focused on nonreceptor tyrosine kinases because PLCγ initiates the calcium signal after tyrosine phosphorylation. Among the nonreceptor tyrosine kinases, genome-wide screening revealed Btk and Tec to be highly expressed in osteoclasts. The Tec kinase family, consisting of Bmx, Btk, Itk, Rlk, and Tec, is preferentially expressed in the hematopoietic system. T cell receptor (TCR) and B cell receptor (BCR) signaling complexes include Itk/Rlk and Tec/Btk, respectively (Schmidt et al., 2004). The role of Btk in antibody production is well recognized by the existence of immunodeficiencies, X-linked agammaglobulinemia (XLA) in humans (Tsukada et al., 1993) and X-linked immunodeficiency (Xid) in mice (Kerner et al., 1995), caused by a mutation in the *Btk* gene; in addition, mice with a combined deficiency of Tec family kinases display both unique and redundant functions in B cells (Btk and Tec) (Ellmeier et al., 2000) and T cells (Itk and Rlk) (Schaeffer et al., 1999). Here we report the crucial role of Btk and Tec in RANKL-induced osteoclastogenesis based on the genetic evidence obtained from $Tec^{-/-}Btk^{-/-}$ mice. In response to RANKL stimulation, Btk and Tec kinases form a signaling complex required for osteoclastogenesis with adaptor molecules such as BLNK, which also recruits Syk, thus linking the RANK and ITAM signals to phosphorylate PLCγ. This study provides a clear example of immunodeficiency association with abnormal bone homeostasis owing to defects in signaling molecules shared by B cells and osteoclasts. Moreover, therapeutic models suggest that suppression of Tec kinases can serve as a molecular basis for the development of future therapeutic strategies against bone diseases.

RESULTS

Osteoclasts Selectively Express Btk and Tec among Tec Kinases

RANK and ITAM signals cooperate to induce calcium signaling, but it has been unknown how these two signals are integrated. To gain insight into the molecules activated by RANKL that are potentially involved in the activation of tyrosine phosphorylation of the PLCγ pathway, we performed a genome-wide screening of mRNAs for nonreceptor tyrosine kinases expressed during osteoclast and osteoblast differentiation (Figure 1A). We identified high expression of *Src* and *Syk*, whose crucial functions in the osteoclast lineage have been well documented (Soriano et al., 1991; Faccio et al., 2003; Koga et al., 2004). Interestingly, osteoclasts, but not osteoblasts, express the mRNAs for *Btk* and *Tec* at a higher level than that for *Src* (Figure 1A). The selective expression of Btk and Tec in osteoclast precursor cells was also confirmed by RT-PCR (Figure 1B) and immunoblot analysis (Figure 1C).

Osteopetrotic Phenotype of Mice Doubly Deficient in Btk and Tec

The results led us to analyze the bone phenotype of mice deficient in Tec (Ellmeier et al., 2000), Btk (Kerner et al., 1995), or both (Ellmeier et al., 2000). Microradiological analysis revealed the trabecular bone volume to be normal in $Tec^{-/-}$ mice, minimally increased in $Btk^{-/-}$ mice, and markedly increased in $Tec^{-/-}Btk^{-/-}$ mice (Figure 1D). Microcomputed tomography clearly indicated that the bone volume was greatly enhanced in $Tec^{-/-}Btk^{-/-}$ mice (Figure 1E). Histological analysis revealed the osteoclast number was significantly reduced in the epiphyseal region, and the bone marrow was abnormally filled with trabecular bone in $Tec^{-/-}Btk^{-/-}$ mice (Figure 1F). We also observed cartilage remnants characteristic of osteopetrosis in $Tec^{-/-}Btk^{-/-}$ mice (Figure 1F). Bone morphometric analysis indicated an increase in bone volume associated with a reduced osteoclast number, a decrease in the indicators of osteoclastic bone resorption (Figure 1G), and a normal level of bone formation in $Tec^{-/-}Btk^{-/-}$ mice (Figure 1H). There was no significant difference in the resorption and formation parameters among the wild-type (WT), $Tec^{-/-}$, and $Btk^{-/-}$ mice (see Figure S1 available online). These results collectively suggest that the increase in bone mass in $Tec^{-/-}Btk^{-/-}$ mice is caused by impaired osteoclastic bone resorption owing to a defect in osteoclast differentiation.

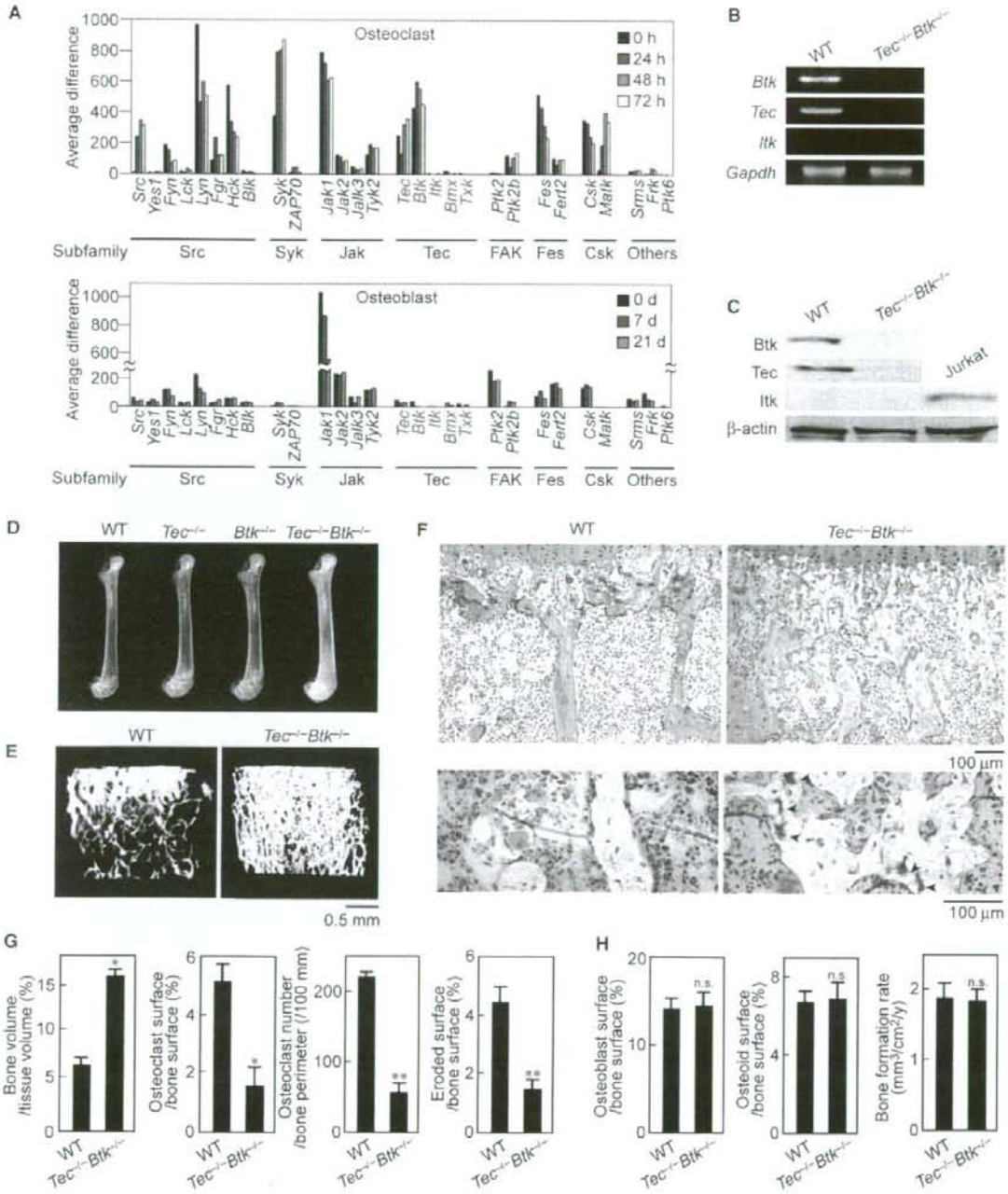

Figure 1. Osteopetrotic Phenotype of *Tec*$^{-/-}$*Btk*$^{-/-}$ Mice

(A) GeneChip analysis of mRNAs for nonreceptor tyrosine kinases during osteoclast and osteoblast differentiation. FAK, focal adhesion kinase; Fes, feline sarcoma oncogene; Csk, c-src tyrosine kinase.

(B) RT-PCR analysis of *Tec*, *Btk*, and *Itk* mRNAs in WT and *Tec*$^{-/-}$*Btk*$^{-/-}$ BMMs.

(C) Expression of Tec, Btk, and Itk proteins in WT and *Tec*$^{-/-}$*Btk*$^{-/-}$ BMMs.

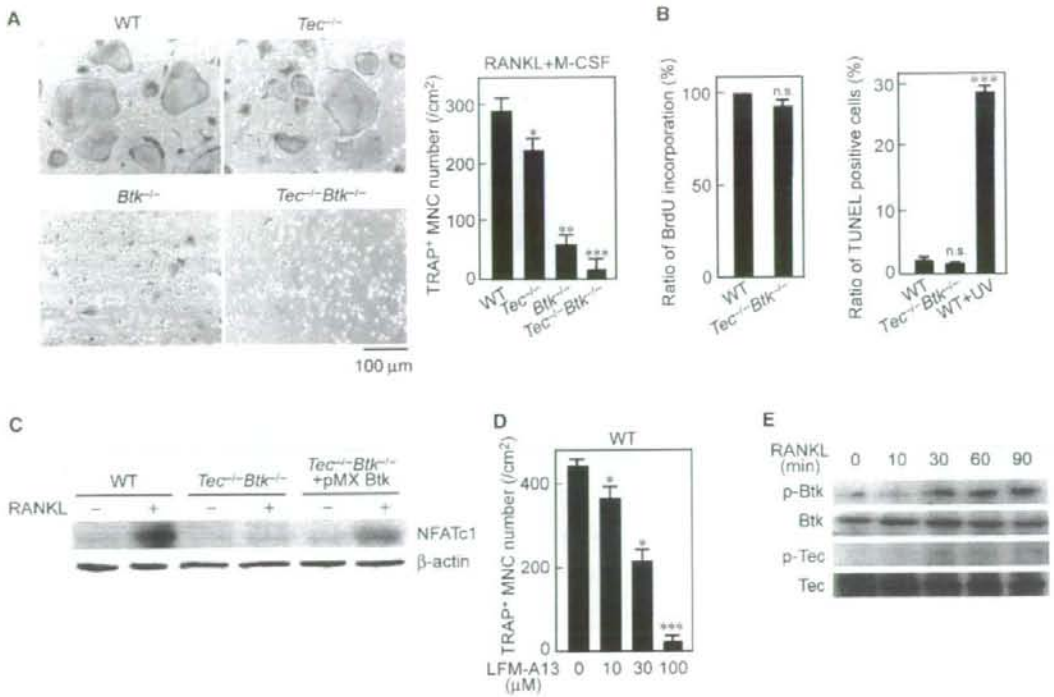

Figure 2. Crucial Role of Tec Family Kinases in RANKL-Induced Osteoclast Differentiation

(A) Osteoclast differentiation from WT, $Tec^{-/-}$, $Btk^{-/-}$, and $Tec^{-/-}Btk^{-/-}$ BMMs in response to RANKL and M-CSF.

(B) Cell proliferation rate (BrdU incorporation assay) and apoptosis (TUNEL assay) of WT and $Tec^{-/-}Btk^{-/-}$ BMMs stimulated with RANKL and M-CSF.

(C) NFATc1 induction in WT and $Tec^{-/-}Btk^{-/-}$ BMMs 72 hr after RANKL stimulation. Retroviral introduction of Btk into $Tec^{-/-}Btk^{-/-}$ BMMs recovers the NFATc1 induction.

(D) Effect of the Tec kinase inhibitor LFM-A13 on the osteoclast differentiation induced by RANKL and M-CSF.

(E) Phosphorylation of Btk and Tec in BMMs in response to RANKL.

Despite the severe defect in osteoclastic bone resorption, the $Tec^{-/-}Btk^{-/-}$ mice had normal tooth eruption, but the results nevertheless suggest that the two kinases play a critically important role in osteoclast differentiation.

Btk and Tec Are Activated by RANKL and Indispensable for Osteoclastogenesis

In vitro osteoclast differentiation was evaluated by counting the multinucleated cells (MNCs) positive for the osteoclast marker tartrate-resistant acid phosphatase (TRAP) after stimulation of BMMs with recombinant RANKL in the presence of M-CSF. Osteoclast differentiation was only minimally affected in $Tec^{-/-}$ cells but was severely impaired in $Btk^{-/-}$ cells and almost completely abrogated in $Tec^{-/-}Btk^{-/-}$ cells (Figure 2A). There was no significant difference in M-CSF-dependent proliferation of precursor cells or the rate of apoptosis between WT and $Tec^{-/-}Btk^{-/-}$ cells (Figure 2B) or in the number of CD11b$^+$ cells in the M-CSF-stimulated bone marrow cells (data not shown). Therefore, there is no defect in the generation of osteoclast precursor cells in $Tec^{-/-}Btk^{-/-}$ mice, although we observed that the survival of mature macrophages derived from $Tec^{-/-}Btk^{-/-}$ mice was partly impaired when cultured with a low concentration of M-CSF (W.E., unpublished data). RANKL-stimulated induction of NFATc1, the key transcription factor for osteoclastogenesis, was severely suppressed in $Tec^{-/-}Btk^{-/-}$ cells (Figure 2C) and $Btk^{-/-}$ cells (data not shown). We also analyzed the effect of the Tec kinase inhibitor LFM-A13 (Mahajan et al., 1999), which was designed to specifically bind the ATP-binding site of Btk,

(D) Microradiograph of the femur of WT, $Tec^{-/-}$, $Btk^{-/-}$, and $Tec^{-/-}Btk^{-/-}$ mice.

(E) Microcomputed tomography of the epiphyseal region of the femurs of WT and $Tec^{-/-}Btk^{-/-}$ mice.

(F) Histological analysis of the proximal tibiae of WT and $Tec^{-/-}Btk^{-/-}$ mice (upper, TRAP/hematoxylin; lower, toluidine blue stainings). Note that the number of TRAP-positive cells is markedly decreased in $Tec^{-/-}Btk^{-/-}$ mice. The bone marrow is filled with unresorbed bone, in which cartilage remnants (arrowheads) characteristic of osteopetrosis are observed.

(G and H) (G) Bone volume and parameters for osteoclastic bone resorption and (H) parameters for osteoblastic bone formation in the bone morphometric analysis of WT and $Tec^{-/-}Btk^{-/-}$ mice. *$p < 0.05$; **$p < 0.01$; ***$p < 0.005$; n.s., not significant (throughout the paper).

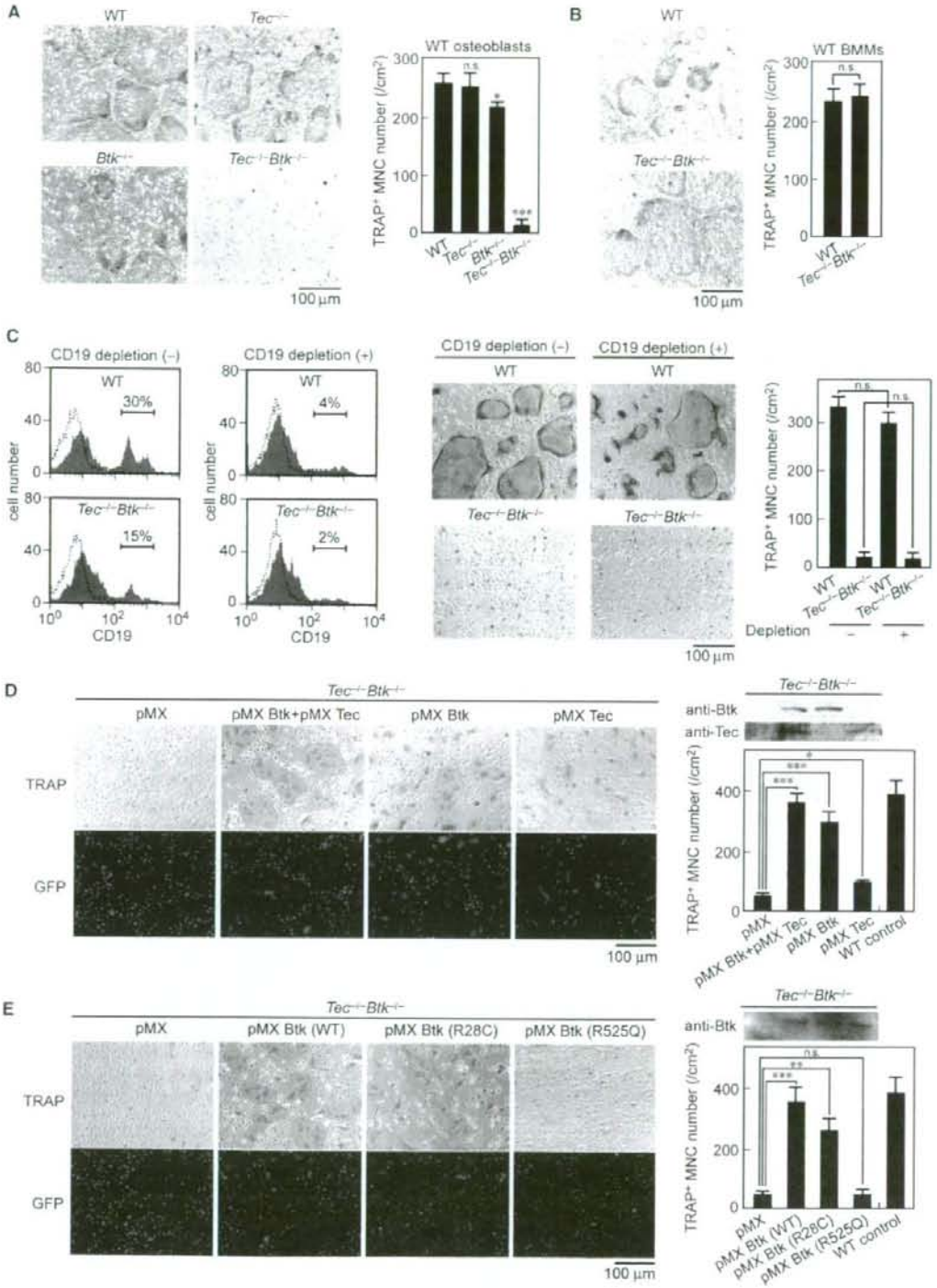
A
WT
Tec−/−
Btk−/−
Tec−/−Btk−/−
100 μm
WT osteoblasts
TRAP+ MNC number (/cm2)
n.s
*
***
WT
Tec−/−
Btk−/−
Tec−/−Btk−/−
B
WT
Tec−/−Btk−/−
100 μm
WT BMMs
TRAP+ MNC number (/cm2)
n.s
WT
Tec−/−Btk−/−
C
CD19 depletion (−)
CD19 depletion (+)
cell number
WT
30%
4%
Tec−/−Btk−/−
15%
2%
CD19
CD19 depletion (−)
CD19 depletion (+)
WT
Tec−/−Btk−/−
100 μm
TRAP+ MNC number (/cm2)
n.s
Depletion
D
Tec−/−Btk−/−
pMX
pMX Btk+pMX Tec
pMX Btk
pMX Tec
TRAP
GFP
100 μm
Tec−/−Btk−/−
anti-Btk
anti-Tec
TRAP+ MNC number (/cm2)
pMX
pMX Btk+pMX Tec
pMX Btk
pMX Tec
WT control
E
Tec−/−Btk−/−
pMX
pMX Btk (WT)
pMX Btk (R28C)
pMX Btk (R525Q)
TRAP
GFP
100 μm
Tec−/−Btk−/−
anti-Btk
TRAP+ MNC number (/cm2)
n.s
pMX
pMX Btk (WT)
pMX Btk (R28C)
pMX Btk (R525Q)
WT control

and which was revealed subsequently to suppress other Tec kinases additionally (Fernandes et al., 2005), on osteoclast differentiation. LFM-A13 strongly inhibited RANKL-induced osteoclastogenesis (Figure 2D) and NFATc1 induction (data not shown). In contrast, this compound only slightly affected the bone resorption activity of osteoclasts (Figure S2). Importantly, phosphorylation of Btk and Tec was induced by RANKL stimulation in BMMs (Figure 2E). Thus, the tyrosine kinases Btk and Tec are activated by RANKL and play a crucial role in RANKL-induced signal transduction during osteoclastogenesis.

Impaired Osteoclastogenesis in *Tec*$^{-/-}$*Btk*$^{-/-}$ Mice Caused by a Cell-Autonomous Mechanism

To determine whether impaired osteoclastogenesis in *Tec*$^{-/-}$*Btk*$^{-/-}$ mice is caused by a cell-autonomous mechanism, we evaluated the osteoclastogenesis in the coculture system of bone marrow cells with osteoblasts. In the coculture of bone marrow cells derived from mutant mice with WT osteoblasts, osteoclast formation was not severely affected in *Tec*$^{-/-}$ or *Btk*$^{-/-}$ cells but was almost abrogated in *Tec*$^{-/-}$*Btk*$^{-/-}$ cells (Figure 3A). In contrast, *Tec*$^{-/-}$*Btk*$^{-/-}$ osteoblasts were normally able to support osteoclastogenesis of WT bone marrow cells (Figure 3B). These results suggest that the impaired osteoclastogenesis in *Tec*$^{-/-}$*Btk*$^{-/-}$ mice is caused by a defect in osteoclast precursor cells. Consistent with the observation that the *Btk*$^{-/-}$ mice have a normal number of osteoclasts in vivo (Figure S1), *Btk*$^{-/-}$ cells differentiate into osteoclasts in the coculture system essentially in a normal manner (Figure 3A), indicating that the larger contribution of Btk is observed only under limited in vitro conditions, including the RANKL/M-CSF-stimulated BMM culture system (Figure 2A). Since a similar observation has been made in *DAP12*$^{-/-}$ cells (Koga et al., 2004), we infer that Btk is more closely associated with the DAP12-dependent pathway.

Since *Tec*$^{-/-}$*Btk*$^{-/-}$ mice have almost no B cells and exhibit severe immunodeficiency (but their T cells are not affected) (Ellmeier et al., 2000), it is possible that the impaired osteoclastogenesis is influenced by differences in the B cell number in the bone marrow. Therefore, we examined whether depletion or addition of CD19$^+$ B cells had any effect on osteoclastogenesis from bone marrow cells containing B cells. Osteoclast differentiation was not influenced by the coexistence of B cells in either WT or *Tec*$^{-/-}$*Btk*$^{-/-}$ cells (Figure 3C). Taken together, these results indicate that the impaired osteoclastogenesis in *Tec*$^{-/-}$*Btk*$^{-/-}$ mice is not related to an abnormality of other cell types such as osteoblasts or B cells, supporting the notion that the impaired osteoclast differentiation is caused by a cell-autonomous mechanism.

Consistent with this notion, retrovirus-mediated expression of Btk and Tec almost completely recovered the osteoclast differentiation in *Tec*$^{-/-}$*Btk*$^{-/-}$ BMMs. The introduction of Btk into *Tec*$^{-/-}$*Btk*$^{-/-}$ BMMs by retroviral transfer markedly rescued the differentiation blockade, but that of Tec rescued it to a lesser extent (Figure 3D). This result is consistent with the dominant role of Btk in osteoclastogenesis in the BMM culture system (Figure 2A). Tec family kinases contain a pleckstrin-homology (PH) domain that binds to phosphatidylinositol-3,4,5-triphosphate (PtdIns[3,4,5]P_3), a lipid product of phosphoinositide 3-kinase, a Tec homology domain, and a carboxyl-terminal kinase domain (Schmidt et al., 2004). A kinase-inactive mutant of Btk (R525Q) that carries a mutation in the kinase domain (Takata and Kurosaki, 1996) did not rescue the osteoclast differentiation blockade, but another mutant (R28C) that harbors a mutation in the PH domain (Takata and Kurosaki, 1996), which causes a certain type of XLA in humans (Tsukada et al., 1993), exhibited a capacity for rescue comparable to the WT Btk (Figure 3E). The results suggest that the function of Btk in osteoclastogenesis requires its kinase activity but does not completely depend on the interaction with PtdIns(3,4,5)P_3 through the PH domain.

Tec Kinases Link the RANK Signal to the Phosphorylation of PLCγ

How does deficiency of Btk and Tec affect the osteoclastogenic signaling pathways? To address these issues by a systems biology approach, we utilized a systematic protein-protein interaction database created by the Genome Network Project (http://genomenetwork.nig.ac.jp/index.html), in which our laboratory has served as a working member. From this database, we extracted the protein-protein interaction network related to the two major signaling pathways regulating osteoclastogenesis, the RANK and ITAM pathways, with which we merged our original data on the increase in mRNA expression after RANKL stimulation (Figure 4A). The RANK-associated gene network included TRAF6, NF-κB, and mitogen-activated protein kinase (MAPK), whereas the ITAM (DAP12/FcRγ)-associated gene network included Syk, PLCγ, and Btk/Tec. As expected, the expression of many RANK-associated molecules was upregulated by RANKL stimulation. Interestingly, the expression of many of the genes in the ITAM-associated gene network was also upregulated by RANKL stimulation.

Based on these results, together with the observation that Btk and Tec were activated by RANKL (Figure 2E), we hypothesized that Btk and Tec are the molecules that bridge the RANK and ITAM pathways to activate calcium signaling. Notably, RANKL-induced tyrosine phosphorylation of PLCγ1 and PLCγ2 was markedly suppressed in *Tec*$^{-/-}$*Btk*$^{-/-}$ cells (Figure 4B). Furthermore, the RANKL-induced calcium oscillation required for *NFATc1* induction was barely observed in *Tec*$^{-/-}$*Btk*$^{-/-}$ cells (Figure 4C). In contrast, we observed a normal level of RANKL-induced activation of MAPKs (ERK, JNK, p38), IκB kinase α (IKKα),

Figure 3. Impaired Osteoclastogenesis in *Tec*$^{-/-}$*Btk*$^{-/-}$ Mice Caused by a Cell-Autonomous Mechanism

(A) Osteoclast differentiation from WT, *Tec*$^{-/-}$, *Btk*$^{-/-}$, and *Tec*$^{-/-}$*Btk*$^{-/-}$ bone marrow cells in the coculture system with WT osteoblasts.

(B) Osteoclast differentiation from WT bone marrow cells in the coculture system with WT or *Tec*$^{-/-}$*Btk*$^{-/-}$ osteoblasts.

(C) Effect of CD19$^+$ B cell depletion on osteoclast differentiation. The number of CD19$^+$ cells before and after depletion of CD19$^+$ B cells in bone marrow cells derived from WT or *Tec*$^{-/-}$*Btk*$^{-/-}$ mice (left). Osteoclast differentiation from WT and *Tec*$^{-/-}$*Btk*$^{-/-}$ BMMs after depletion of CD19$^+$ B cells in response to RANKL and M-CSF (right).

(D) Effects of retroviral expression of Tec (pMX Tec) and/or Btk (pMX Btk) on osteoclastogenesis from *Tec*$^{-/-}$*Btk*$^{-/-}$ BMMs stimulated with RANKL and M-CSF.

(E) Effects of retroviral expression of WT Btk or Btk mutants harboring a mutation in the PH domain (R28C) or the kinase domain (R525Q) on osteoclastogenesis from *Tec*$^{-/-}$*Btk*$^{-/-}$ BMMs stimulated with RANKL and M-CSF.

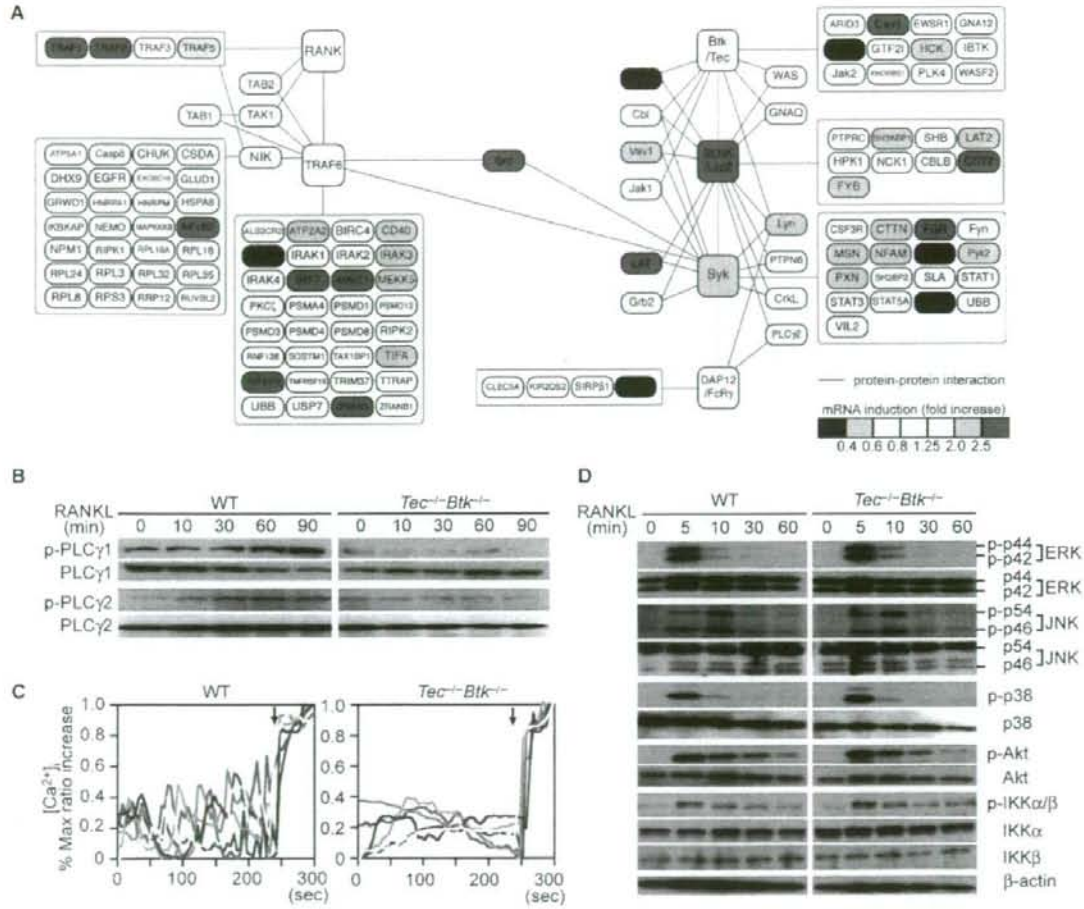

Figure 4. Tec Kinases Mediate Osteoclastogenic Signaling Pathway

(A) Dynamic protein-protein interaction network in osteoclast differentiation. Proteins connected with a black line are interacting partners, and the color indicates how many fold mRNA expression was increased 24 hr after RANKL stimulation.

(B) RANKL-induced PLCγ1 and PLCγ2 phosphorylation in WT and *Tec*$^{-/-}$*Btk*$^{-/-}$ BMMs.

(C) Oscillatory change in the intracellular Ca^{2+} concentration in WT and *Tec*$^{-/-}$*Btk*$^{-/-}$ BMMs after RANKL stimulation. The addition of 10 μM ionomycin at the end of each experiment is indicated by an arrow. Each color indicates a different cell in the same field.

(D) RANKL-induced ERK, JNK, p38, Akt, and IKK phosphorylation in WT and *Tec*$^{-/-}$*Btk*$^{-/-}$ BMMs.

IKKβ, and Akt, all of which are activated downstream of TRAF6 (Wong et al., 1999) (Figure 4D). These results indicate that RANKL-activated Btk and Tec are selectively involved in the phosphorylation of PLCγ, and a defect in calcium signaling causes the impaired *NFATc1* induction in *Tec*$^{-/-}$*Btk*$^{-/-}$ cells. Thus, Btk and Tec link the RANK signal to calcium signaling in the osteoclast lineage.

Tec Kinases Form an Osteoclastogenic Signaling Complex with Scaffold Proteins

Since PLCγ activation is known to be dependent on the ITAM signal, another question arises as to how PLCγ activation is regulated by both RANK and ITAM signals. The ITAM-associated gene network indicates that ITAM associates with Syk, which associates with and phosphorylates scaffold proteins such as BLNK (Ishiai et al., 1999). Because BLNK associates with Btk in a phosphorylation-dependent manner in B cells (Hashimoto et al., 1999), we examined whether RANKL-activated Btk is recruited to BLNK in BMMs. The colocalization of Btk and BLNK was increased, at what appeared to be the plasma membrane, after RANKL stimulation (Figure 5A and Figure S3). This translocation was not observed in *DAP12*$^{-/-}$*FcRγ*$^{-/-}$ cells (Figure 5A and Figure S3), suggesting that the ITAM signals are also required for the formation of the Btk-BLNK complex. Consistent with this, immunoblot analysis showed that Btk coimmunoprecipitated with BLNK in BMMs in the presence of RANKL, but

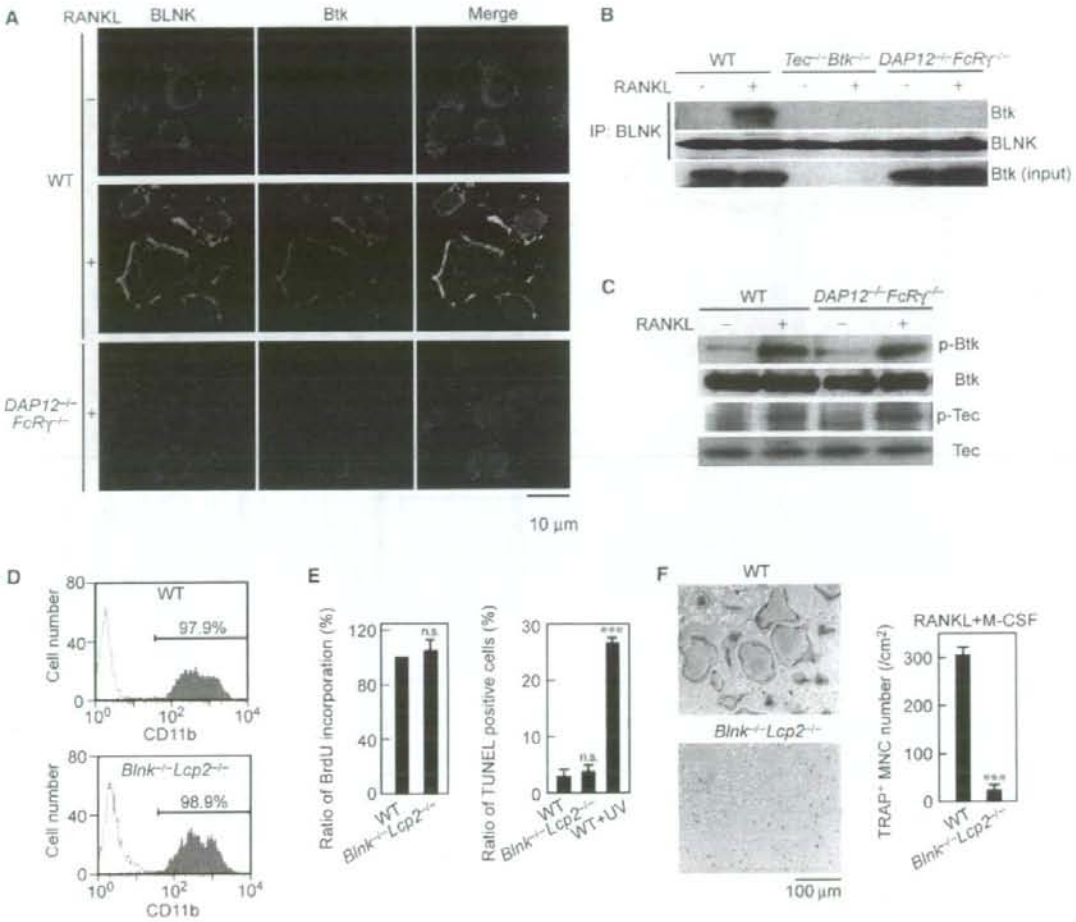

Figure 5. Tec Kinases Form an Osteoclastogenic Signaling Complex with Scaffold Proteins

(A) Immunofluorescence microscopic analysis of colocalization of Btk and BLNK in WT and *DAP12*$^{-/-}$*FcRγ*$^{-/-}$ cells 15 min after RANKL stimulation. The nuclei were stained with Hoechst 33342.

(B) Immunoprecipitation analysis of the interaction between Btk and BLNK in WT and *DAP12*$^{-/-}$*FcRγ*$^{-/-}$ cells 15 min after RANKL stimulation.

(C) Tyrosine phosphorylation of Tec kinases in WT and *DAP12*$^{-/-}$*FcRγ*$^{-/-}$ cells 15 min after RANKL stimulation.

(D) Expression of CD11b in the M-CSF-stimulated bone marrow cells from WT and *Blnk*$^{-/-}$*Lcp2*$^{-/-}$ mice (flow cytometry).

(E) Cell proliferation rate (BrdU incorporation assay) and apoptosis (TUNEL assay) of WT and *Blnk*$^{-/-}$*Lcp2*$^{-/-}$ BMMs stimulated with RANKL and M-CSF.

(F) Osteoclast differentiation from WT and *Blnk*$^{-/-}$*Lcp2*$^{-/-}$ BMMs in response to RANKL and M-CSF.

the association was abrogated in *DAP12*$^{-/-}$*FcRγ*$^{-/-}$ cells (Figure 5B). Furthermore, Tec kinases were phosphorylated in response to RANKL, even in *DAP12*$^{-/-}$*FcRγ*$^{-/-}$ cells (Figure 5C). Thus, the activation of Btk by RANK and the activation of BLNK by the ITAM signal are both required for the association of Btk with BLNK, which may function as the molecular switch that integrates RANK and ITAM signals.

To further investigate the role of BLNK in osteoclastogenesis, we analyzed osteoclast differentiation in BMMs derived from *Blnk*$^{-/-}$ mice (Hayashi et al., 2003). However, there was no significant difference in RANKL-induced osteoclastogenesis between the WT and *Blnk*$^{-/-}$ cells (data not shown), suggesting that another molecule(s) compensates for the loss of BLNK. SLP-76 (encoded by *Lcp2*) is an adaptor protein homologous to BLNK, functioning mainly in T cells (Pivniouk and Geha, 2000). Since there was no significant difference in RANKL-induced osteoclastogenesis between the WT and *Lcp2*$^{-/-}$ cells (data not shown), we analyzed mice doubly deficient in BLNK and SLP-76 (*Blnk*$^{-/-}$*Lcp2*$^{-/-}$ mice). Although *Blnk*$^{-/-}$ mice frequently develop acute leukemia (Jumaa et al., 2003), there was a normal number of CD11b^{+} osteoclast precursor cells in the M-CSF-stimulated bone marrow cells from *Blnk*$^{-/-}$*Lcp2*$^{-/-}$ mice (Figure 5D), and